Analytic nuclear gradients of the algebraic-diagrammatic construction scheme for the polarization propagator up to third order of perturbation theory

Dirk R. Rehn (iD), and Andreas Dreuw (iD)

View Online   Export Citation   CrossMark

ARTICLES YOU MAY BE INTERESTED IN

Analytic nuclear gradients of the algebraic-diagrammatic construction scheme for the polarization propagator up to third order of perturbation theory

View Online   Export Citation   CrossMark

Dirk R. Rehn[a] [ID] and Andreas Dreuw[b] [ID]

AFFILIATIONS

Interdisciplinary Center for Scientific Computing and Physical-Chemistry Institute, Ruprecht-Karls University,
Im Neuenheimer Feld 205, 69120 Heidelberg, Germany

[a] Electronic mail: rehn@uni-heidelberg.de
[b] Electronic mail: dreuw@uni-heidelberg.de. URL: http://www.iwr.uni-heidelberg.de/groups/compchem/.

ABSTRACT

Analytic gradient expressions for the algebraic diagrammatic construction (ADC) scheme for the polarization propagator up to third order are derived using a Lagrangian approach. An implementation within the Q-CHEM electronic structure package for excited-state nuclear gradients of the ADC(2), ADC(2)-x, and ADC(3) models based on restricted and unrestricted Hartree–Fock references is presented. Details of the implementation and the applicability of the newly derived gradients for geometry optimizations and the quality of the resulting structures are discussed.

Published under license by AIP Publishing. https://doi.org/10.1063/1.5085117

I. INTRODUCTION

Since the early work of Pulay,[1] energy derivatives have become a key tool for the quantum chemical description of various optical phenomena and the understanding of chemical reactions. As Pulay wrote in a recent review article:[2] "Analytical calculation of energy derivatives with respect to nuclear coordinates revolutionized applied molecular quantum mechanics by allowing the routine calculation of molecular structures and related properties." The efficient evaluation of energy derivatives using analytical derivative techniques is an important trait for quantum chemical methods since energy derivatives are needed in almost all *in silico* quantum chemical studies. In general, the investigation of potential energy surfaces (PESs) is one of the most prominent examples for the use of derivatives with respect to nuclear coordinates. The efficient localization of characteristic stationary points on PESs like minima and maxima corresponding to stable isomers and transition states, respectively, or minimum energy pathways describing chemical reactions connects quantum chemical calculations with real-life chemistry. This is true for thermal, mostly ground-state chemistry,

as well as photochemistry occurring in excited electronic states. Also in the latter cases, exploration of excited state PESs with the help of analytic nuclear gradients leads straightforwardly to insight into, for instance, fluorescence properties, nonadiabatic transitions, and conical intersections.

Recently, the second-order algebraic diagrammatic construction method [ADC(2)][3,4] for the polarization propagator has gained more attention due to its computational efficiency and reliability for organic molecules with a single-reference electronic ground state. A promising method for the description of electronically excited-states of medium-sized organic molecules is the third order ADC method [ADC(3)],[5,6] which has been demonstrated recently to possess the accuracy of the approximate third-order coupled cluster (CC3) method[7] in the description of vertical excitation energies of organic molecules at lower computational effort. The total energies of the excited states within a given ADC method are given as the sum of its excitation energy and the ground state Møller-Plesset[8] energy of the respective order. Thus, excited-state potential energy surfaces at the ADC(2) or ADC(3) level inevitably inherit the limitations of the parent MP(2) or MP(3) method.

It should be noted that gradients of any energy functional can simply be obtained via finite differences for each component of the perturbation. However, the applicability of numerical derivatives of quantum chemical energy functionals is strongly limited for different reasons. A limiting factor for numerical differentiation is the required number of single point energy calculation of at least two points for each component of the perturbation. If the perturbation is a geometrical distortion and the system has N atoms, then (in the absence of symmetry) at least $3N - 5$ single point energy calculations have to be performed, one at the starting geometry and one along each degree of freedom. Additionally, numerical differentiation suffers from numerical instabilities which can lead to slow or failing convergence. In contrast to finite differences, analytical derivatives are numerically stable and can be performed at a computational cost comparable to a single energy calculation for many quantum chemical methods.[2]

The derivation of analytical gradients in quantum chemical methods is based on the realization of Hellmann and Feynman,[9,10] the so-called Hellmann-Feynman theorem, that the derivative of the energy $\langle \Psi | \hat{H} | \Psi \rangle$ of the exact wavefunction $| \Psi \rangle$ with respect to an external perturbation ξ can be obtained as the expectation value of the perturbed Hamiltonian. For approximate wavefunctions, the first term on the right-hand side (rhs) of Eq. (1), the so-called Hellmann-Feynman term, is in many cases a good approximation of the total derivative. However, additional contributions enter the total derivative

$$\frac{dE}{d\xi} = \langle \Psi | \frac{\partial \hat{H}}{\partial \xi} | \Psi \rangle + \frac{\partial \langle \Psi | \hat{H} | \Psi \rangle}{\partial \Delta} \frac{d\Delta}{d\xi} \quad (1)$$

due to the chain rule. These arise from the dependence of the energy on nonvariational parameters Δ. The in general very cumbersome evaluation of these non-Hellman-Feynman contributions can be circumvented as shown by Handy and Schäfer using the so-called Z-vector method.[11] A generalization and rigorous derivation of this Z-vector method is the Lagrangian formalism, which has become the standard method for the derivation of analytical gradients in quantum chemistry.[2,12] The Lagrangian technique involves the introduction of the Lagrangian energy functional

$$\mathcal{L} = E + \sum_i \kappa_i f_i(\boldsymbol{\Delta}) \quad (2)$$

and the undetermined Lagrange multipliers $\{\kappa_i\}$. The conditions $\{f_i(\boldsymbol{\Delta}) = 0\}$ are chosen such that the Lagrangian is stationary with respect to the Lagrange multipliers. By requiring that the Lagrangian is additionally stationary with respect to all nonvariational parameters of the original energy functional, conditional equations for the Lagrange multipliers are obtained. Once the Lagrange multipliers are determined by solving these conditional equations, the Lagrangian fulfills the Hellmann-Feynman theorem, and by evaluating its partial derivative the total derivative of the original energy functional can be obtained.

Today, analytical derivatives for several excited state methods are available and extensively used for the investigation of molecular photochemistry. For example, analytical derivatives have been realized for the semiempirical multireference configuration interaction method OM2/MRCI[13,14] as well as for standard MRCI,[15] which allow nowadays for efficient excited-state surface hopping dynamics.[16,17] Also for density functional

theory (DFT)-based methods like time-dependent DFT (TDDFT),[18–20] analytic derivatives are available.[21–24] In the context of *ab initio* wavefunction-based approaches, analytic nuclear gradients exist, for example, for the complete-active-space size-consistent field (CASSCF) method,[25–29] the complete-active-space perturbation theory of second-order (CASPT2),[30,31] the approximate second-order coupled-cluster model CC2,[7,32–35] or the equation of motion and linear-response coupled-cluster methods EOM-/LR-CCSD.[36–43] Also, for ADC(2), analytic excited-state gradients have already been realized.[34]

In this paper, the Lagrangian formalism is used to derive analytical expressions for energy derivatives of the ADC approach of the polarization propagator up to third order. For the first time, analytical derivative expressions for the extended second order ADC model [ADC(2)-x][3] and the third order ADC(3) are presented. Extending the procedure for the computation of analytical energy derivatives for ADC(2) to the ADC(2)-x model requires only few additional modifications. By contrast, the ADC(3) energy contains additional parameters from the perturbation theoretical treatment, which require the introduction of additional terms in the Lagrangian. After the general Lagrangian for ADC models is introduced, the expressions for the amplitude response for models up to ADC(3) are presented. How the expressions for the density matrices can be derived is briefly demonstrated for the expressions of ADC(2), and the results for all models are collected in the Appendix.

II. THEORY AND IMPLEMENTATION

A. The ADC energy expression

The central equation in an ADC scheme of a particular propagator is the Hermitian eigenvalue problem

$$\mathbf{MX} = \mathbf{X\Omega}, \quad (3)$$

which needs to be solved. In the case of ADC for the polarization propagator, the so-called ADC matrix $\mathbf{M}$ has originally been derived as a "nondiagonal" matrix representation of the polarization propagator $\Pi_{pq,rs} = \Pi^+_{pq,rs} + \Pi^-_{pq,rs}$ which has in the spectral representation the form

$$\Pi_{pq,rs}(\omega) = \sum_{n \neq 0} \left(\frac{\langle \Psi_0 | \hat{c}^\dagger_q \hat{c}_p | \Psi_n \rangle \langle \Psi_n | \hat{c}^\dagger_r \hat{c}_s | \Psi_0 \rangle}{\omega - (E_n - E_0)} \right) + \Pi^-_{pq,rs}(\omega). \quad (4)$$

Here, $| \Psi_0 \rangle$ denotes the electronic ground state wavefunction with the corresponding energy E_0, $\hat{c}^\dagger_q$ and $\hat{c}_q$ are creation (and annihilation) operators defined with respect to the Hartree–Fock (HF) reference. The summation on the rhs of Eq. (4) is carried out over all electronically excited states $| \Psi_n \rangle$ with respective energies E_n. The ADC approach postulates the existence of a representation

$$\Pi_{pq,rs}(\omega) = \mathbf{F}^\dagger (\mathbb{1}\omega - \mathbf{M})^{-1} \mathbf{F} + \Pi^-_{pq,rs}(\omega). \quad (5)$$

The excitation energies $\{\omega_n = E_n - E_0\}$ can be found as poles of $\Pi^+_{pq,rs}$, which yields Eq. (3), where $\boldsymbol{\Omega}$ is a diagonal matrix of the excitation energies and $\mathbf{X}$ is a unitary matrix of the eigenvectors x_n of the ADC matrix and connects the ADC representation of the polarization propagator to the "diagonal" form. Additionally,

transition properties can be obtained through the so-called "modified transition amplitudes" **F**.

Originally, the expressions of the ADC matrix have been obtained by comparing a perturbation expansion of the polarization propagator with a series expansion of **M**

$$\mathbf{M} = \mathbf{M}^{(0)} + \mathbf{M}^{(1)} + \mathbf{M}^{(2)} + \cdots. \tag{6}$$

The diagrammatic analysis of the perturbation expansion of the polarization propagator using the MP partitioning[8] leads to algebraic expressions for the matrix elements of **M**.

An alternative route to the ADC matrix equation is offered by the so-called intermediate state representation (ISR).[44] Here, the matrix **M** is identified as a representation of the ground-state-energy-shifted electronic Hamiltonian H of the molecular system in the orthonormal basis of so-called intermediate states $\{|\tilde{\Psi}_I\rangle\}$,

$$\mathbf{M}_{IJ} = \langle \tilde{\Psi}_I | H - E_0 | \tilde{\Psi}_J \rangle = \langle \tilde{\Psi}_I | H | \tilde{\Psi}_J \rangle - \delta_{IJ} E_0. \tag{7}$$

The intermediate states are constructed from so-called correlated excited states $|\Psi_0^I\rangle$, which are formed by letting excitation operators $\{\hat{C}_I\}$ act on the exact ground state wavefunction. The successive orthonormalization with respect to the ground state and each other using the Gram-Schmidt procedure yields the intermediate states

$$|\Psi_0^I\rangle = \hat{C}_I |\Psi_0\rangle \xrightarrow{\text{GS}} |\tilde{\Psi}_I\rangle. \tag{8}$$

To obtain the ADC matrix expressions, the intermediate states are constructed as indicated in Eq. (8) and the exact ground state wavefunction and energy are replaced by series expansions

$$|\Psi_0\rangle = |\Psi_0\rangle^{(0)} + |\Psi_0\rangle^{(1)} + |\Psi_0\rangle^{(2)} + \cdots, \tag{9}$$

$$E_0 = E_0^{(0)} + E_0^{(1)} + E_0^{(2)} + \cdots. \tag{10}$$

Again by using the MP-splitting of the Hamiltonian and collecting terms up to the respective order of a given ADC model, the identical algebraic expressions are obtained as in the original derivation. Following the ISR concept yields two major results which exceed the original derivation of the ADC expressions using propagator theory. First of all, the ISR offers an efficient and convenient way to calculate excited-state and transition properties since every operator, e.g., the dipole operator, can be represented in the intermediate state basis. Second, absolute energies can be obtained as eigenvalues of the representation of the unshifted Hamiltonian in the intermediate state basis

$$\tilde{\mathbf{M}}_{IJ} = \langle \tilde{\Psi}_I | H | \tilde{\Psi}_J \rangle = \mathbf{M}_{IJ} + \delta_{IJ} E_0, \tag{11}$$

which are given as

$$E_n = x_n^\dagger \tilde{\mathbf{M}} x_n = x_n^\dagger \mathbf{M} x_n + E_0 = \omega_n + E_0. \tag{12}$$

Thus, the ground state energy corresponding to a given ADC(N) model is given by the ground state MP(N) energy.

B. ADC Lagrangian and analytic energy derivatives

As given in Eq. (12), the total ADC energy E_n of an excited state depends on the eigenvector x_n and the parameters stemming from the MP-expansion of the wavefunction and energy, which will be

called **T** in the following. In addition, E_n depends on the parameters from the reference state $|\Psi_0\rangle^{(0)}$ and the elements $\{C_{\mu p}\}$ of the orbital transformation matrix **C**, which transforms from atomic orbitals $\{\chi_\mu\}$ to molecular orbitals $\{\phi_p\}$,

$$\phi_P = \sum_\mu C_{\mu p} \chi_\mu. \tag{13}$$

The total derivative of $E(x, \mathbf{T}, \mathbf{C})$ with respect to a perturbation ξ is given as

$$\frac{dE}{d\xi} = \frac{\partial E}{\partial \xi} + \frac{\partial E}{\partial x}\frac{dx}{d\xi} + \frac{\partial E}{\partial \mathbf{T}}\frac{d\mathbf{T}}{d\xi} + \frac{\partial E}{\partial \mathbf{C}}\frac{d\mathbf{C}}{d\xi}, \tag{14}$$

where the index n has been dropped for brevity. The first thing to note is that the second term on the rhs of Eq. (14) vanishes since the excitation energy is stationary with respect to the eigenvector. From the remaining three contributions to the total derivative, the first term, the so-called Hellmann-Feynman term, can, in principle, directly be evaluated in a straightforward way from the perturbed Hamiltonian. This is done by contracting the one- and two-particle density matrices with the derivative of the one- and two-electron integrals ($h_{pq} = \langle p | \hat{h} | q \rangle$ and $\langle pq || rs \rangle$)

$$\frac{\partial E}{\partial \xi} = \sum_{pq} h_{pq}^\xi \gamma_{pq} + \frac{1}{4} \sum_{pqrs} \langle pq || rs \rangle^\xi \Gamma_{pqrs}. \tag{15}$$

More demanding is the evaluation of the two remaining terms, i.e., the dependence of the parameters with respect to the perturbation. However, the so-called amplitude and orbital response contributions, $\frac{d\mathbf{T}}{d\xi}$ and $\frac{d\mathbf{C}}{d\xi}$, respectively, can be avoided and the total derivative can be obtained in a convenient and efficient way offered by the Lagrangian method.

As first realized by Handy and Schaefer,[11] the total derivative can be evaluated for all post-Hartree–Fock methods, including ADC, in the same way as the partial derivative and requires in addition only a set of Lagrange multipliers $\Theta = \{\theta_{pq}\}$ and the derivative of the overlap matrix $\mathbf{S} = \{S_{pq}\} = \{\langle \phi_p | \phi_q \rangle\}$ of the molecular orbitals, which can be obtained by transforming from the AO basis,

$$\frac{\partial S_{pq}}{\partial \xi} = S_{pq}^\xi = \sum_{\mu\nu} C_{\mu p} S_{\mu\nu}^\xi C_{\nu q}. \tag{16}$$

By introducing effective one- and two-particle density matrices γ^e and Γ^e, the total derivative can be written as

$$\frac{dE}{d\xi} = \sum_{pq} h_{pq}^\xi \gamma_{pq}^e + \frac{1}{4} \sum_{pqrs} \langle pq || rs \rangle^\xi \Gamma_{pqrs}^e + \sum_{pq} \theta_{pq} S_{pq}^\xi. \tag{17}$$

Three different parts contribute to the effective density matrices in Eq. (17), and their explicit form can be derived using the Lagrange formalism. Generally, a Lagrangian for wavefunction-based methods can be used to avoid the computation of partial derivatives with respect to nonoptimized wavefunction parameters. It can be constructed using the conditions for the equations of the underlying reference state and the correlation treatment. If canonical Hartree–Fock is used, the Fock matrix $\mathbf{F} = \{f_{pq}\}$ is diagonal and the overlap matrix **S** is the unity matrix, which can be expressed as

$$f_{pq} - \delta_{pq}\epsilon_p = 0 \quad \text{and} \quad S_{pq} - \delta_{pq} = 0. \tag{18}$$

In the same way, $\{f_z\}$ are equations that satisfy the condition

$$f_z(t_z) = 0 \tag{19}$$

for the parameters of the MP perturbation expansion (or in general the correlation treatment) $\mathbf{T} = \{t_z\}$. Using Eqs. (18) and (19), a general Lagrangian for methods based on canonical Hartree–Fock (restricted and unrestricted) can be constructed as[36]

$$L(\mathbf{C}, \mathbf{T}, \boldsymbol{\Lambda}, \boldsymbol{\Theta}, \tilde{\boldsymbol{T}}) = E(\mathbf{C}, \mathbf{T}) + \sum_{pq} \lambda_{pq}(f_{pq} - \delta_{pq}\epsilon_p)$$
$$+ \sum_{pq} \omega_{pq}(S_{pq} - \delta_{pq}) + \sum_z \tilde{t}_z f_z(t_z). \tag{20}$$

Here, $\boldsymbol{\Lambda} = \{\lambda_{pq}\}$ and $\tilde{\boldsymbol{T}} = \{\tilde{t}_z\}$ are additional sets of undetermined Lagrange multipliers. It should be noted that the Lagrange multiplier matrices $\boldsymbol{\Lambda}$ and $\boldsymbol{\Theta}$ are symmetric. The additional terms besides the energy are zero, if the conditions of Eqs. (18) and (19) are satisfied.

From the definition of the Lagrangian L follows directly that it is stationary with respect to the Lagrange multipliers

$$\frac{\partial L}{\partial \lambda_{pq}} = f_{pq} - \delta_{pq}\epsilon_p = 0,$$
$$\frac{\partial L}{\partial \omega_{pq}} = S_{pq} - \delta_{pq} = 0, \tag{21}$$
$$\frac{\partial L}{\partial t_z} = f_z(t_z) = 0.$$

The undetermined Lagrange multipliers can be chosen freely and are defined by imposing

$$\frac{\partial L}{\partial \mathbf{C}} \overset{!}{=} 0 \tag{22}$$

and

$$\frac{\partial L}{\partial \mathbf{T}} \overset{!}{=} 0, \tag{23}$$

meaning that L is stationary with respect to all nonvariational parameters. Thus, the Lagrangian is stationary with respect to all wavefunction parameters (and Lagrange multipliers) and the total derivative of L becomes equal to the partial derivative. From the definition of L in Eq. (20) follows that the total derivative of the energy E with respect to a perturbation ξ is given by

$$\frac{dE}{d\xi} = \frac{dL}{d\xi} \overset{!}{=} \frac{\partial L}{\partial \xi}, \tag{24}$$

if the Lagrange multipliers satisfy Eqs. (22) and (23).

The partial derivative of L with respect to ξ is given by

$$\frac{\partial L}{\partial \xi} = \frac{\partial E}{\partial \xi} + \sum_{pq} \lambda_{pq} \frac{\partial f_{pq}}{\partial \xi} + \sum_{pq} \omega_{pq} \frac{\partial S_{pq}}{\partial \xi} + \sum_i \tilde{t}_i \frac{\partial f_i(t_i)}{\partial \xi} \tag{25}$$

and can be sorted and rewritten as

$$\frac{\partial L}{\partial \xi} = \sum_{pq} h_{pq}^{\xi}\big(\gamma_{pq}(T) + \gamma_{pq}^{O}(\Lambda) + \gamma_{pq}^{A}(\tilde{T})\big)$$
$$+ \frac{1}{4} \sum_{pqrs} \langle pq \| rs \rangle^{\xi}\big(\Gamma_{pqrs}(T) + \Gamma_{pqrs}^{O}(\Lambda) + \Gamma_{pqrs}^{A}(\tilde{T})\big)$$
$$+ \sum_{pq} \omega_{pq} S_{pq}^{\xi}. \tag{26}$$

By comparison with Eq. (26), the effective density matrices occurring in Eq. (17) can be identified as

$$\gamma^e = \gamma(\mathbf{T}) + \gamma^{O}(\boldsymbol{\Lambda}) + \gamma^{A}(\tilde{\boldsymbol{T}}) \tag{27}$$

and

$$\Gamma^e = \Gamma(\mathbf{T}) + \Gamma^{O}(\boldsymbol{\Lambda}) + \Gamma^{A}(\tilde{\boldsymbol{T}}). \tag{28}$$

The so-called unrelaxed densities $\gamma(\mathbf{T})$ and $\Gamma(\mathbf{T})$ are identical to those in Eq. (15) and depend on the parameters of the correlation treatment. Both remaining terms on the rhs of Eqs. (27) and (28) depend on the Lagrange multipliers. The orbital response contributions, $\gamma^{O}(\boldsymbol{\Lambda})$ and $\Gamma^{O}(\boldsymbol{\Lambda})$, depend on the set of Lagrange multipliers, which guarantees stationarity of the Lagrangian with respect to changes in the parameters of the orbital basis. Their explicit form is method-independent, and its derivation is only briefly reviewed in Sec. II C. A detailed derivation can be found in the work of Levchenko et al.[36] The method-dependent amplitude response contributions, $\gamma^{A}(\tilde{\boldsymbol{T}})$ and $\Gamma^{A}(\tilde{\boldsymbol{T}})$, depend on the Lagrange multipliers ensuring stationarity of L with respect to the parameters of the correlation treatment. Their explicit form is discussed for each model individually in Sec. II D.

C. Orbital response expressions

To determine the orbital response Lagrange multipliers, a system of linear equations has to be solved, determined by the imposed condition given in Eq. (22). This system of linear equations can be derived starting from the definition of the Lagrangian in Eq. (20),

$$L = E + \sum_{pq} \lambda_{pq}(f_{pq} - \delta_{pq}\epsilon_p) + \sum_{pq} \omega_{pq}(S_{pq} - \delta_{pq}) + \sum_z \tilde{t}_z f_z(t_z). \tag{29}$$

It is useful to express the energy, using the relation between the Fock matrix

$$f_{pq} = h_{pq} + \sum_i \langle pi \| qi \rangle \tag{30}$$

and the core Hamiltonian h_{pq}, as

$$E = \sum_{pq} f_{pq} \tilde{\gamma}_{pq} + \frac{1}{4} \sum_{pqrs} \langle pq \| rs \rangle \tilde{\Gamma}_{pqsr}. \tag{31}$$

The introduced densities $\tilde{\gamma}$ and $\tilde{\Gamma}$ are identified as

$$\tilde{\gamma}_{pq} = \gamma_{pq}, \tag{32}$$
$$\tilde{\Gamma}_{pqrs} = \Gamma_{pqrs} - \gamma_{ps}\delta_{qr}\delta_{q\in\text{occ.}} + \gamma_{pr}\delta_{qs}\delta_{q\in\text{occ.}} + \gamma_{qs}\delta_{pr}\delta_{p\in\text{occ.}} - \gamma_{qr}\delta_{ps}\delta_{p\in\text{occ.}}. \tag{33}$$

Here, $\tilde{\Gamma}$ is the so-called nonseparable part of the two-particle density matrix and $\delta_{p\in\text{occ.}}$ means that the nonseparable density matrix has only nonzero blocks where p is an occupied index. In the same way, the explicit form of the orbital response contributions can be identified as

$$\gamma_{pq}^O = \lambda_{pq}, \tag{34}$$

$$\Gamma_{pqrs}^O = 2\left(-\lambda_{ps}\delta_{qr}\delta_{q\in\text{occ.}} + \lambda_{pr}\delta_{qs}\delta_{q\in\text{occ.}} + \lambda_{qs}\delta_{pr}\delta_{p\in\text{occ.}} - \lambda_{qr}\delta_{ps}\delta_{p\in\text{occ.}}\right). \tag{35}$$

The Lagrangian is sorted, collecting all contributions besides the orbital response Lagrange multipliers in

$$\gamma'(\mathbf{T},\tilde{\mathbf{T}}) = \gamma(\mathbf{T}) + \gamma^A(\tilde{\mathbf{T}}) \text{ and } \Gamma'(\mathbf{T},\tilde{\mathbf{T}}) = \tilde{\Gamma}(\mathbf{T}) + \Gamma^A(\tilde{\mathbf{T}}) \tag{36}$$

and, thus, written as

$$L = \sum_{pq} f_{pq}\gamma'_{pq} + \frac{1}{4}\sum_{pqrs}\langle pq||rs\rangle\Gamma'_{pqrs} + \sum_{pq}\lambda_{pq}(f_{pq} - \delta_{pq}\epsilon_p) + \sum_{pq}\omega_{pq}S_{pq}. \tag{37}$$

Now, the partial derivatives with respect to the elements of the orbital transformation matrix $\mathbf{C}$ are evaluated. The Lagrangian depends on the elements of $\mathbf{C}$ through the Fock matrix, the two-electron integrals, and the overlap matrix. The system of linear equations according to Eq. (22) has the form

$$0 = \sum_{pq}\frac{\partial f_{pq}}{\partial C_{\mu p}}(\gamma'_{pq} + \lambda_{pq}) + \frac{1}{4}\sum_{pqrs}\frac{\partial\langle pq||rs\rangle}{\partial C_{\mu p}}\Gamma'_{pqrs} + \sum_{pq}\omega_{pq}\frac{\partial S_{pq}}{\partial C_{\mu p}}. \tag{38}$$

To obtain programmable expressions from Eq. (38) and to avoid expressions with partially transformed integrals,

$$\frac{\partial L}{\partial C_{\mu p}} = 0 \tag{39}$$

is replaced by

$$\sum_{\mu}C_{\mu q}\frac{\partial L}{C_{\mu p}} = 0, \tag{40}$$

and the partial derivatives are performed. Evaluation of the required derivatives of the Fock matrix, the two-electron integrals, and the overlap matrix is straightforward.[36] Equation (39) yields

$$0 = \sum_{\mu}C_{\mu u}\frac{\partial L}{\partial C_{\mu t}}$$

$$= \sum_{pq}\left(\lambda_{pq} + \gamma'_{pq}\right)\left(\delta_{pt}f_{uq} + \delta_{qt}f_{pu} + (\langle pu||qt\rangle + \langle pt||qu\rangle)\delta_{t\in\text{occ.}}\right)$$

$$+ \sum_{pqr}\frac{1}{2}\left(\Gamma'_{tpqr}\langle up||qr\rangle + \Gamma'_{qrtp}\langle qr||up\rangle\right)$$

$$+ \sum_{pq}\omega_{pq}\left(\delta_{pt}S_{uq} + \delta_{qt}S_{pu}\right), \tag{41}$$

which can be simplified by assuming real two-electron integrals and using $f_{pq} = \epsilon_p\delta_{pq}$, $S_{pq} = \delta_{pq}$, as well as the symmetry of $\mathbf{\Lambda}$ and $\mathbf{\Omega}$ to arrive at

$$0 = \sum_{\mu}C_{\mu u}\frac{\partial L}{\partial C_{\mu t}}$$

$$= 2\left(\lambda_{tu} + \gamma'_{tu}\right)\epsilon_u + \sum_{pq}\left(\gamma'_{pq} + \lambda_{pq}\right)\left(\langle pu||qt\rangle\delta_{t\in\text{occ.}}\right)$$

$$+ \sum_{pqr}\Gamma'_{tpqr}\langle up||qr\rangle + 2\omega_{ut}. \tag{42}$$

Choosing the indices t and u in Eq. (42) from different orbital spaces, respectively, enables the decoupling of $\mathbf{\Lambda}$ and $\mathbf{\Omega}$. Throughout this paper, indices $i,j,k,\ldots$ refer to occupied orbitals and indices $a,b,c,\ldots$ refer to virtual orbitals,

$$0 = \sum_{\mu}C_{\mu i}\frac{\partial L}{\partial C_{\mu a}} - \sum_{\mu}C_{\mu a}\frac{\partial L}{\partial C_{\mu i}}$$

$$= 2\left(\lambda_{ia} + \gamma''_{ia}\right)(\epsilon_i - \epsilon_a) + \sum_{pq}\left(\lambda_{pq} + \gamma''_{pq}\right)(\langle pa||qi\rangle - \langle pi||qa\rangle)$$

$$+ \sum_{pqr}\left(\Gamma''_{ipqr}\langle ap||qr\rangle - \Gamma''_{apqr}\langle ip||qr\rangle\right). \tag{43}$$

If no approximations restricting the active orbital space are employed, λ_{ij} and λ_{ab} are zero since the energy is invariant with respect to orbital rotations within the space of occupied or virtual orbitals. However, for frozen core or frozen virtual approximations, λ_{ij} and λ_{ab} can be obtained through the equations,

$$0 = \sum_{\mu}C_{\mu i}\frac{\partial L}{\partial C_{\mu j}} - \sum_{\mu}C_{\mu j}\frac{\partial L}{\partial C_{\mu i}} \text{ and } 0 = \sum_{\mu}C_{\mu a}\frac{\partial L}{\partial C_{\mu b}} - \sum_{\mu}C_{\mu b}\frac{\partial L}{\partial C_{\mu a}} \tag{44}$$

and then enter Eq. (43).

It should be noted that the contributions from the Hartree–Fock energy to Eq. (43) cancel and, thus, γ' and Γ' are replaced by

$$\gamma''_{pq} = \gamma'_{pq} - \delta_{pq}\delta_{p\in\text{occ.}} \quad \text{and}$$

$$\Gamma''_{pqrs} = \Gamma'_{pqrs} + \delta_{ps}\delta_{qr}\delta_{p\in\text{occ.}}\delta_{q\in\text{occ.}} - \delta_{pr}\delta_{qs}\delta_{p\in\text{occ.}}\delta_{q\in\text{occ.}}. \tag{45}$$

After the occupied-virtual block of $\mathbf{\Lambda}$ has been determined iteratively, Eq. (42) can be used to determine $\mathbf{\Omega}$.

D. Amplitude response expressions

The total ADC energy E of an excited state in terms of the excited state vector $x = \left(x_{ia}, x_{ijab,\ldots}\right)^T$ is given as

$$E = E_0^{MP} + \omega^{ADC} = E_0^{MP} + x^\dagger\mathbf{M}x. \tag{46}$$

A general Lagrangian for the total energy at a given ADC(n) level for $n\geqslant 1$ is thus constructed as

$$L^{ADC(n)} = E_{HF} + \sum_{i>1}^N\left(E^{(i)} + x^\dagger\mathbf{M}^{(i)}x\right) + R_A^{ADC(N)} + R_O(\mathbf{\Lambda},\mathbf{\Omega})$$

$$= E_{HF} + \sum_{pq}f_{pq}\gamma_{pq}^N + \frac{1}{4}\sum_{pqrs}\langle pq||rs\rangle\Gamma_{pqrs}^N + R_O(\mathbf{\Lambda},\mathbf{\Omega}) \tag{47}$$

with the orbital response contributions collected in

$$R_O(\mathbf{\Lambda}, \mathbf{\Omega}) = \sum_{pq} \lambda_{pq}(f_{pq} - \delta_{pq}\epsilon_p) + \sum_{pq} \omega_{pq} S_{pq}. \quad (48)$$

The Lagrange multipliers and conditions R_A, i.e., the amplitude response contribution, ensure stationarity with respect to parameters originating from the perturbation treatment occurring in the ADC(N) matrix and $E_0^{MP(N)}$. These are the so-called t-amplitudes for MP(2), ADC(2), and ADC(2)-x, additionally the T^D-amplitudes for MP(3), and furthermore the second order ground state density correction $\rho^{(2)}$ for ADC(3). For the ADC(0–1) schemes, the total energy of an excited state depends only on the parameters of the underlying reference state and the excitation vector, and thus, no additional Lagrange multipliers are required. The explicit form of the amplitude response contribution for MP and ADC models up to third order is given here,

$$R_A^{ADC(0)} = R_A^{ADC(1)} = 0, \quad (49)$$

$$R_A^{ADC(2)} = R_A^{ADC(2)-x} = \sum_{ijab} \bar{t}_{ijab} f(t_{ijab}) = R_A^{MP(2)}, \quad (50)$$

$$R_A^{MP(3)} = \sum_{ijab} \bar{t}_{ijab} f(t_{ijab}) + \sum_{ijab} \bar{T}_{ijab}^D g(T_{ijab}^D)$$

$$= R_A^{MP(2)} + \sum_{ijab} \bar{T}_{ijab}^D g(T_{ijab}^D), \quad (51)$$

$$R_A^{ADC(3)} = \sum_{ijab} \bar{t}_{ijab} f(t_{ijab}) + \sum_{ijab} \bar{T}_{ijab}^D g(T_{ijab}^D) + \sum_{pq} \bar{\rho}_{pq} h(\rho_{pq}^{(2)})$$

$$= R_A^{MP(3)} + \sum_{pq} \bar{\rho}_{pq} h(\rho_{pq}^{(2)}). \quad (52)$$

These amplitude response contributions depend on the parameters contained in the MP perturbation expansions

$$t_{ijab} = \frac{\langle ij||ab \rangle}{\epsilon_a + \epsilon_b - \epsilon_i - \epsilon_j}, \quad (53)$$

$$T_{ijab}^D = \frac{\sum_{kc} t_{ikac}\langle kb||jc \rangle - \frac{1}{2}\left(\sum_{cd} t_{ijcd}\langle ab||cd \rangle + \sum_{kl} t_{klab}\langle ij||kl \rangle\right)}{\epsilon_a + \epsilon_b - \epsilon_i - \epsilon_j}$$

$$= \frac{I_{ijab}^T}{\epsilon_a + \epsilon_b - \epsilon_i - \epsilon_j}, \quad (54)$$

$$\rho_{ia}^{(2)} = -\frac{1}{2\epsilon_a - \epsilon_i}\left(\sum_{jbc} t_{ijab}\langle ja||bc \rangle + t_{jkab}\sum_{jkb}\langle jk||ib \rangle\right) = \frac{I_{ia}^\rho}{\epsilon_a - \epsilon_i}. \quad (55)$$

Here, the intermediates I_{ijab}^T and I_{ia}^ρ have been introduced as shorthand notation. In this work, the second order MP correction to the ground state density matrix is used in the ADC(3) matrix and the stationarity of the Lagrangian with respect to the occupied-occupied and virtual-virtual blocks of $\rho^{(2)}$ is guaranteed through the Lagrange multipliers $\{\bar{t}\}$ since they contain only products of t-amplitudes. However, for the occupied-virtual part, additional Lagrange multipliers $\{\bar{\rho}_{ia}\}$ are required. If higher-order corrections for the one-particle ground state density are employed, e.g., using the so-called Dyson expansion method (DEM),[45] different side conditions have to be included in the Lagrangian.

The conditions for the amplitude response equation for each parameter set follow directly from their definition as

$$0 = f(t_{ijab}) = t_{ijab}(\epsilon_a + \epsilon_b - \epsilon_i - \epsilon_j) - \langle ij||ab \rangle, \quad (56)$$

$$0 = g(T_{ijab}^D) = T_{ijab}^D(\epsilon_a + \epsilon_b - \epsilon_i - \epsilon_j) - I_{ijab}^T, \quad (57)$$

$$0 = h(\rho_{ia}^{(2)}) = \rho_{ia}^{(2)}(\epsilon_a - \epsilon_i) - I_{ia}^\rho. \quad (58)$$

Once the Lagrange multipliers are obtained, the amplitude-relaxed density matrices can be straightforwardly computed. The explicit form of these density matrices γ^N and Γ^N is identified for each ADC(N) model by comparison of the left- and right-hand sides of

$$\sum_{i>1}^N \left(E^{(i)} + x^\dagger \mathbf{M}^{(i)} x\right) + R_A^{ADC(N)} = \sum_{pq} f_{pq}\gamma_{pq}^N + \frac{1}{4}\sum_{pqrs}\langle pq||rs \rangle \Gamma_{pqrs}^N. \quad (59)$$

To obtain the numerical equations for the Lagrange multipliers, the partial derivative of the Lagrangian with respect to each parameter set has to be evaluated.

As mentioned already above, in the ADC(2) and ADC(2)-x schemes, the only nonvariational parameters are the t-amplitudes besides the parameters of the reference state. Evaluating the partial derivative of the respective Lagrangian

$$0 = \frac{\partial L}{\partial t_{ijab}} = \frac{\partial\left(E^{(2)} + \omega^{ADC(2)}\right)}{\partial t_{ijab}} + \frac{\partial \sum_{klcd}\bar{t}_{klcd} f(t_{klcd})}{\partial t_{ijab}}$$

$$= -\langle ij||ab \rangle + \frac{\partial \omega^{ADC(2)}}{\partial t_{ijab}} + \bar{t}_{ijab}(\epsilon_a + \epsilon_b - \epsilon_i - \epsilon_j) \quad (60)$$

yields the numerical equations for the Lagrange multipliers, which reads

$$\bar{t}_{ijab}^{ADC(2)} = t_{ijab} - \frac{\frac{\partial \omega^{ADC(2)}}{\partial t_{ijab}}}{\epsilon_a + \epsilon_a - \epsilon_i - \epsilon_j}. \quad (61)$$

It should be noted that for MP(2), the Lagrange multipliers $\{\bar{t}\}$ do not need to be computed separately since they are equivalent to the t-amplitudes.[46] The partial derivative of the ADC(2) excitation energy with respect to the t-amplitudes yields (for details, see the Appendix)

$$\frac{\partial \omega^{ADC(2)}}{\partial t_{ijab}} = (1 - \hat{\mathcal{P}}_{ab})\sum_c \langle ij||bc \rangle \sum_k x_{ka} x_{kc}$$

$$- (1 - \hat{\mathcal{P}}_{ij})\sum_k \langle jk||ab \rangle \sum_c x_{ic} x_{kc}$$

$$- (1 - \hat{\mathcal{P}}_{ij})(1 - \hat{\mathcal{P}}_{ab}) x_{ia} \sum_{ck}\langle jk||bc \rangle x_{kc}. \quad (62)$$

Here, the permutation operator $\hat{P}_{pq}$ has been introduced which interchanges indices p and q.

In the ADC(3) scheme, the amplitude response contains two additional sets of Lagrange multipliers besides the t-amplitudes. Since the determining equations for $\{\bar{t}\}$ depend on the Lagrange multipliers for the T^D-amplitudes and the second order one-particle density $\rho^{(2)}$, these last two sets of Lagrange multipliers must be computed first according to

$$\bar{T}_{ijab}^D = t_{ijab} - \frac{\frac{\partial \omega^{ADC(3)}}{\partial T_{ijab}^D}}{\epsilon_a + \epsilon_a - \epsilon_i - \epsilon_j}. \tag{63}$$

Similar to MP(2), the Lagrange multipliers $\{\bar{T}^D\}$ do not have to be computed separately for MP(3) since they can be replaced by the scaled t-amplitudes.[47] The T^D-amplitudes enter the ADC(3) matrix at the same positions as the t-amplitudes enter the ADC(2) matrix, and thus the partial derivative of the ADC(3) excitation energy with respect to the T^D-amplitudes yields the same expression as in Eq. (62)

$$\frac{\partial \omega^{ADC(3)}}{\partial T_{ijab}^D} \cong \frac{\partial \omega^{ADC(2)}}{\partial t_{ijab}}. \tag{64}$$

By evaluating the partial derivative of L with respect to the occupied-virtual part of $\rho^{(2)}$, the equations for the Lagrange multipliers $\bar{\rho}_{ia}$ are determined via

$$\bar{\rho}_{ia} = \frac{-\frac{\partial \omega^{ADC(3)}}{\partial \rho_{ia}^{(2)}}}{\epsilon_a - \epsilon_i} = \frac{2}{\epsilon_a - \epsilon_i}\left(-\sum_{jk}\langle ij||ka\rangle \sum_c x_{jc}x_{kc} + \sum_{jb}x_{jb}\sum_k \langle ij||kb\rangle x_{ka} \right.$$
$$\left. -\sum_{bc}\langle ic||ab\rangle \sum_k x_{kb}x_{kc} + \sum_{jb}x_{jb}\sum_c \langle jc||ab\rangle x_{ic} \right). \tag{65}$$

For ADC(3), the expressions determining $\bar{t}$ are sorted into four different parts, i.e.,

$$\bar{t}_{ijab}^{ADC(3)} = t_{ijab} + \frac{\sum_{n=1}^6 {}^n\bar{t}_{ijab} + \bar{t}_{ijab}^{T^D} + \bar{t}_{ijab}^\rho}{\epsilon_a + \epsilon_b - \epsilon_i - \epsilon_j}. \tag{66}$$

The first term on the rhs of Eq. (66), the t-amplitudes, stems from the second order contribution to the ground state energy. The second term is the partial derivative of ω with respect to the t-amplitudes again split into six contributions from different canonical blocks of the two-particle density matrix. The remaining contributions arise from the partial derivatives of the equations determining T^D and $\rho_{ia}^{(2)}$. Explicit expressions for the terms in Eq. (66) can be found in the Appendix.

E. Implementation

The analytical energy derivatives have been implemented in a development version of the quantum chemical program package Q-Chem 4.4.[48] All implementations have been integrated in the `adcman` module,[49] which is a C++ project containing different variants of ADC and which can in principle be integrated into other quantum chemical programs as well due to the modular structure of `adcman` and the related libraries. The implementation relies on the open-source tensor library `libtensor`,[50] which handles all algebraic operations using optimized linear algebra routines at its core. It splits large tensors into smaller blocks, which are stored on different levels of memory, i.e., core memory and disk-space, enabling parallel algorithms. In addition, `libtensor` provides a convenient interface facilitating straightforward implementations of tensor expressions. It treats symmetries which are encountered in quantum

chemical calculations, i.e., permutation and spin symmetry as well as point-group symmetry.

The evaluation of analytical energy derivatives is performed following the same algorithm for all implemented ADC models. First, the eigenvalue problem of the respective ADC matrix is solved using the Davidson algorithm.[51] In the next step, the amplitude Lagrange multipliers are computed. In the case of ADC(3), the Lagrange multipliers for the MP(2) density and the T^D-amplitudes have to be evaluated first because they are required for the computation of the t-amplitude Lagrange multipliers. Successively, the amplitude-relaxed one- and two-particle density matrices are computed, which are used as input for the orbital response. The orbital response Lagrange multipliers are found as the solution of a system of linear equations, which is solved using the DIIS algorithm.[52] In the last step, the fully relaxed density matrices and the overlap Lagrange multipliers are transformed into the AO basis and contracted with the perturbed integrals and overlap matrix to obtain the energy derivative.

To validate the correct derivation and implementation of the analytic derivatives, a comparison with numerical derivatives has been made.[53] A compilation of results for numerical and analytical derivatives can be found in the supplementary material.

III. APPLICATIONS

To test the accuracy and elucidate the range of applicability of the newly derived analytic nuclear gradients of the ADC schemes of the polarization propagator up to third order, three different classes of molecules have been chosen and the equilibrium geometries of their excited singlet S_1 states have been computed. All excited-state optimizations have been performed using the implementation presented in this work. In the following, equilibrium distances in the first excited singlet state of the three diatomic molecules N_2, BF, and CO have been calculated since highly accurate experimental as well as theoretical reference data are available. To compare with existing results at the ADC(2) level from the literature,[34] the equilibrium distances have been obtained using the aug-cc-pwCVQZ basis set.[54–56] As the second test, the equilibrium structures of two small organic molecules, *s-trans*-butadiene (butadiene) and *s-trans*-acrolein (acrolein) (Fig. 1), in the excited S_1 state are computed, for which CASPT2 reference data are available. For direct comparison, butadiene and acrolein have been optimized at ADC levels using the 6-31G* basis set enforcing C2h and C$_S$ point group symmetry, respectively.

As the third example, the vertical fluorescence and absorption energies of *s-trans*-(2,2$'$)-bithiophene (BT) (Fig. 1) have been calculated and are compared to experimental results. Oligothiophenes play important roles in medical and technical applications, and their derivatives are often used as electron donors in the field of organic solar cells[57–59] and as imaging agents for the detection of β-amyloid protein deposits,[60] which are the main effectors in Alzheimer's disease. The key mechanism, which can also be studied in the bithiophene molecule, is the planarization of the otherwise nonplanar bithiophene upon electronic excitation. It is accompanied by a significant Stokes shift of the fluorescence wavelength and induces conformational changes in its molecular environment. For the simulation of the Stokes shift, the equilibrium structure
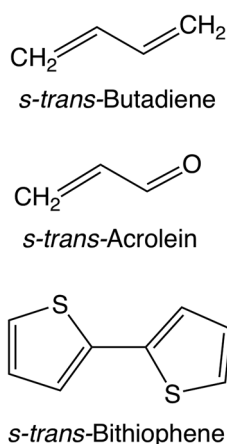
FIG. 1. Molecular structure of test molecules, for which high-quality data for the excited-state equilibrium geometries is available for comparison.

of the first excited singlet state of bithiophene has been computed at ADC levels using the cc-pVDZ basis set and enforcing C_2 symmetry.

A. Excited-state interatomic distances in diatomics

The first and simplest test of the accuracy of the nuclear gradients of ADC methods is performed for the interatomic distances in the diatomics N_2, CO, and BF. In Table I, the equilibrium interatomic distances for the lowest excited singlet state of these diatomics obtained at ADC levels are compared to the theoretical values obtained at EOM-CCSD and CC3 levels[34] as well as with experimental ones.[61] A detailed comparison for interatomic distances between ADC(2) and CC2 equilibrium structures is already available in the literature[34] and thus omitted here.

Overall, CC3 shows clearly the best agreement for the three calculated intermolecular distances of the S_1 states compared with the experimental data. ADC(3) and CCSD underestimate the equilibrium intermolecular distances, while ADC(2) and ADC(2)-x overestimate them. ADC(2) shows the largest errors, and in all three cases, ADC(2)-x improves over the ADC(2) results. For the first excited $^1\Sigma_u$ state of N_2, ADC(3) yields results with an accuracy comparable

to CC3, while CCSD underestimates the bond lengths by 0.027 Å. All ADC models show the largest error for the first excited $^1\Pi$ state of CO. ADC(2) largely overestimates the excited-state bond lengths by 0.043 Å, while ADC(3) underestimates it by 0.025 Å. For the BF molecule, ADC(2) and ADC(2)-x yield identical values overestimating the equilibrium distance of the $^1\Pi$ excited state by 0.008 Å; by contrast, ADC(3) underestimates it by approximately the same amount of 0.010 Å.

B. Excited-state equilibrium geometries of s-trans-butadiene and s-trans-acrolein

As the first test for organic molecules, the equilibrium structures of s-trans-butadiene in the primarily single excited $1^1B_u^+$ and the primarily doubly excited $2^1A_g^-$ have been optimized at ADC levels and compared to CASPT2 reference data. The bond lengths and angles of the excited-state equilibrium structure are summarized in Table II. For the singly excited $1^1B_u^+$ state of butadiene, the optimized geometrical parameters of the equilibrium structure are very similar at all ADC levels and close to those obtained by CASPT2. The single bonds are obtained as 1.399 Å at the CASPT2 level and as 1.397 Å in the ADC(2) and ADC(3) structure. ADC(2)-x yields a length for the single bonds of 1.400 Å. At the CASPT2 level, the original double bonds are 0.022 Å longer than the original central single bond at the equilibrium structure of the $1^1B_g^+$ state. This effect of bond-length inversion in this state is slightly more pronounced at the ADC(2) and ADC(3) levels (0.027 Å), as well as in the ADC(2)-x optimized equilibrium structure (0.025 Å).

In general, the $2^1A_g^-$ state of s-trans-butadiene and linear all-trans-polyenes is recognized as notoriously difficult to be described correctly by electronic structure methods. For this predominantly doubly excited state, the single bond length of the equilibrium structures is again very similar at ADC(2) and ADC(3) levels, both with 1.399 Å, and 1.401 Å at the CASPT2 level. Only ADC(2)-x gives a smaller value of 1.381 Å. However, the bond-length inversion is generally larger in the $2^1A_g^-$ state compared to the $1^1B_u^+$ state due to the double-excitation character of the former. Compared to the CASPT2 equilibrium structure, the inversion pattern is described qualitatively differently by ADC(2) compared to

TABLE I. Comparison of the equilibrium distances of the first excited singlet states of the three isoelectronic diatomic molecules N_2, CO, and BF computed at ADC levels compared to the values obtained at CCSD and CC3 levels. For these calculations, the aug-cc-pwCVQZ basis set has been used.

		ADC(2)	ADC(2)-x	ADC(3)	CCSD[a]	CC3[a]	Expt.[b]
N_2	$^1\Sigma_u^-$	1.290	1.288	1.272	1.248	1.280	1.275
CO	$^1\Pi$	1.278	1.250	1.210	1.222	1.245	1.235
BF	$^1\Pi$	1.312	1.312	1.294	1.301	1.307	1.304

[a]Reference 34.
[b]Reference 61.

TABLE II. Excited state equilibrium bond lengths and angles in Å and degrees for the first two excited states of butadiene. The ADC results have been obtained using the 6-31G* basis set, and CASPT2 results are taken from Ref. 62.

	CASPT2[a]	ADC(2)	ADC(2)-x	ADC(3)
$1^1B_u^+\ \pi \to \pi*$				
C=C	1.421	1.424	1.425	1.424
C—C	1.399	1.397	1.400	1.397
∠ C=C—C	124.1	124.9	124.7	124.7
$2^1A_g^-\ \pi \to \pi*$				
C=C	1.500	1.488	1.563	1.543
C—C	1.401	1.399	1.381	1.399
∠ C=C—C	123.3	121.3	124.3	124.0

[a]Reference 62.

ADC(2)-x and ADC(3). This different behavior has its origin in the different perturbation-theoretical treatment of doubly excited states. While doubly excited states are described correctly only at zeroth order on ADC(2), at ADC(2)-x and ADC(3) levels, they are correct up to first order. As a consequence, ADC(2) underestimates the difference between single and double bond lengths with 0.089 Å in the $2^1A_g^-$ state with only 0.089 Å, while ADC(2)-x and ADC(3) overestimate it with 0.183 Å and 0.144 Å, respectively, compared to CASPT2.

Turning to acrolein as the second organic test molecule, the computed bond lengths and angles of the equilibrium structure of acrolein for the first excited state $1^1A''$ are given in Table III. In this case, the largest difference in the geometrical parameters obtained at different ADC models is observed for the carbon-oxygen bond length. Compared to the CASPT2 structure which has a C—O bond length of 1.345 Å, ADC(2) and ADC(2)-x (1.392 overestimate the carbon-oxygen bond length to be 1.425 and 1.392 Å, respectively. As in the case of CO, ADC(3) underestimates also this C—O bond lengths with 1.300 Å. Considering the C—C bond lengths, CASPT2 describes the single bond slightly shorter with 1.384 Å compared to 1.393 Å for the carbon-carbon double bond in the $1^1A''$ state. For both ADC(2) and ADC(2)-x structures, the C—C double bond is longer than the single bond in the excited state. However, while the difference in length is the same as for CASPT2 and ADC(2) with 0.009 Å, in the case of ADC(2)-x, it is significantly larger with 0.059 Å. In contrast to ADC(2) and ADC(2)-x, ADC(3) describes the changes in the carbon-carbon bonds qualitatively different compared to CASPT2. Here, the bond length of the double bond is shorter than the single bond by 0.015 Å.

C. Fluorescence of *s-trans*-(2,2′)-bithiophene

As the third example, the equilibrium geometry of *s-trans*-(2,2′)-bithiophene (BT) has been optimized in the first excited 1^1B_1 singlet state at ADC levels and the corresponding fluorescence energy has been calculated. The 1^1B_1 excited singlet state has predominantly single excitation character and is essentially characterized as one-electron transition from the highest occupied into the lowest unoccupied molecular orbital. The obtained geometrical parameters for the equilibrium structure of BT are compiled in Table IV together with those obtained previously at the CASSCF(12,10)/cc-pVDZ level[63] for the 1^1B_1 state and those for the

TABLE III. Excited state equilibrium bond lengths and angles in Å and degrees for the first excited state $1^1A''$ of acrolein obtained using ADC(2)-x, ADC(3), and CASPT2 using the 6-31G* basis set.

	CASPT2[a]	ADC(2)	ADC(2)-x	ADC(3)
	$1^1A''$ $n \rightarrow \pi*$			
C=O	1.345	1.425	1.392	1.300
C—C	1.384	1.376	1.359	1.400
C=C	1.393	1.385	1.418	1.385
∠ C=C—C	122.1	121.9	122.9	124.4
∠ C—C=O	125.2	125.3	124.4	124.3

[a]Reference 62.

TABLE IV. Parameters of the first excited state 1^1B_1 equilibrium structure of *s-trans*-(2,2′)-bithiophene in Å and degrees obtained using ADC(2), ADC(2)-x, ADC(3), and CASSCF(12,10) using the cc-pVDZ basis set compared to those of the MP(2)/def-TZVPP ground state equilibrium structure.

	MP (2)[a]	CASSCF (12,10)[b]	ADC (2)	ADC (2)-x	ADC (3)
	1^1A_1		1^1B_1 $\pi \rightarrow \pi*$		
∠ S—C₂—C₂′—S′	150.1	180.0[c]	180.0	180.0	180.0
∠ S—C₂—C₂′	120.7	...	119.5	119.1	120.3
∠ C₂—S—C₅	92.7	...	90.9	91.1	90.8
S—C₂	1.714	1.768	1.792	1.788	1.786
S—C₅	1.702	1.739	1.728	1.728	1.734
C₂—C₂′	1.445	1.378	1.388	1.390	1.392
C₂—C₃	1.385	1.446	1.444	1.446	1.443
C₃—C₄	1.407	1.401	1.395	1.398	1.397
C₄—C₅	1.377	1.405	1.414	1.417	1.408

[a]MP(2)/def-TZVPP.
[b]Reference 63.
[c]Angle of 180° enforced by C₂ᵥ symmetry.

electronic ground state computed at the MP2 level. BT is not planar in the electronic ground state and exhibits a central dihedral angle of about 150° at the MP2 level; however, it is known to planarize upon electronic excitation.[60] All excited state methods, ADC as well as CASSCF, reproduce this planarization of BT in the first excited state, and the obtained equilibrium structure of the 1^1B_1 state has C₂ᵥ symmetry. Overall, all computed bond lengths of the equilibrium structures at all three tested ADC levels agree very favorably and differ by less than 0.01 Å. Also, CASSCF yields a very similar excited-state equilibrium geometry and the largest difference compared to the ADC structures is found in the sulfur-carbon bond S—C₂ of about 0.02 Å.

To relate the optimized S₁ equilibrium structures of BT to an experimental observable, vertical absorption and fluorescence energies, as well as the resulting Stokes shifts, have been computed at all ADC levels, which are compiled in Table V. The corresponding

TABLE V. Vertical absorption and fluorescence energies (in eV) with the corresponding oscillator strengths as well as the Stokes shift for the 1^1B_1 state of *s-trans*-(2,2′)-bithiophene at ADC(2), ADC(2)-x, and ADC(3) levels using the cc-pVDZ basis set compared to experimental values.

	ADC (2)	ADC (2)-x	ADC (3)	Exp.
	1^1B_1 $\pi \rightarrow \pi*$			
Vertical absorption	4.74	4.14	4.58	4.13[a], 3.86 (0-0)[a]
f_{osc}	0.47	0.36	0.43	
Vertical fluorescence	3.81	3.23	3.63	3.40[b]
f_{osc}	0.50	0.38	0.45	
Stokes shift	0.93	0.91	0.95	0.46–0.73

[a]Reference 64.
[b]Reference 65.

absorption energies have been obtained at the MP2/def2-TZVPP ground state structure, and the Stokes shift is defined as the difference between the absorption and fluorescence energy.

The calculated absorption and fluorescence energies at the ADC levels show the typical behavior previously observed for ADC(2), ADC(2)-x, and ADC(3).[6] ADC(2) overestimates the vertical excitation energies, while ADC(2)-x excitation energies are substantially smaller and ADC(3) results lie usually in between. In detail, the computed vertical absorption energies are 4.74, 4.14, and 4.58 eV at ADC(2), ADC(2)-x, and ADC(3) levels of theory, and also the computed fluorescence energies follow the same trend with 3.81, 3.23, and 3.63 eV, respectively. In comparison with the experimental values, ADC(2)-x seems to be the most accurate; however, the computed vertical energies do not directly correspond to the experimental values because vibrational and environmental effects are not included. In addition, a rather small basis set has been used for these first proof-of-principle calculations. However, the experimentally observed large Stokes shift of about 0.7 eV is well reasonably reproduced by all ADC models with 0.91–0.95 eV, considering the limitations mentioned above.

IV. DISCUSSION

In general, it is difficult to judge the quality of excited state equilibrium structures since reliable experimental values are often not available. However, in the case of the three tested diatomic molecules N_2, CO, and BF, experimental data are available and a thorough evaluation is possible. ADC(2) and ADC(2)-x turned out to overestimate the equilibrium interatomic distances of the first excited electronic states. In the case of these three diatomics, going from ADC(2) to ADC(2)-x improves the results most likely due to the higher-order treatment of double excitations at the ADC(2)-x level. Going to ADC(3), the equilibrium distances are underestimated with the approximately same absolute error as ADC(2)-x for all three diatomics. The fact that ADC(3) does not perform better than ADC(2)-x may be attributed to the underlying MP(2) and MP(3) ground state methods since the ADC total energies inherit their problems. In fact, MP(3) is well known generally not to yield a systematic improvement over MP(2).[66] For the tested diatomics, MP(3) yields indeed too short ground state equilibrium distances in the case of CO with a bigger absolute error than MP(2) which yields too long bond distances, explaining the behavior of the ADC methods for the excited state structures.

For the first excited state, bright $1^1B_u^+$ state of butadiene, which has predominantly single excitation character, ADC(2) and ADC(3) yield identical results, which are also very similar to those obtained at ADC(2)-x and CASPT2 levels. For the primarily doubly excited $2^1A_g^-$ state, ADC(2) yields a qualitatively different equilibrium structure than ADC(2)-x and ADC(3), which is certainly due to the higher-order description of doubly excited states at the latter two levels. However, compared to CASPT2, ADC(2)-x and ADC(3) overestimate the bond-length inversion at the $2^1A_g^-$ equilibrium structure, which is caused by two major factors. First, in particular, ADC(2)-x and also still ADC(3) overestimate the amount of double-excitation character of the $2^1A_g^-$ state. Second, due to the large geometrical changes of the excited-state structure compared to the ground-state structure, accompanied by a significant change

in bond-order, MP(2) and MP(3) do not necessarily provide an accurate description of the ground state at the excited-state minimum structure.

In the case of acrolein, the different ground-state methods MP2 and MP3 as well as the different treatment of the double excitations in the description of the $1^1A''$ state lead to qualitative different results at the three different levels of ADC(2), ADC(2)-x, and ADC(3). Here, it is hard to judge whether CASPT2 yields a better description than ADC(3). However, ADC(2) is reasonable to assume to yield a too long C=O carbonyl bond and ADC(2)-x to overestimate bond-length inversion in the carbon-carbon bonds due to the overestimation of its double excitation character.

Similar to the first excited state of butadiene, all three ADC models yield a very similar description of the equilibrium structure of the first excited 1^1B_1 state of bithiophene. This is on the one hand due to the pure single-excitation character of this excited state and the comparable small changes in the geometrical parameter in the excited state compared to the ground state on the other. Although the planarization of the central dihedral angle in the excited state leads to a strong Stokes shift, the ground state description by MP2 or MP3 does not break down because the degree of multireference character does not increase along with the geometric relaxation in the excited state. Hence, all ADC methods yield similar results.

V. SUMMARY AND CONCLUSIONS

In this work, analytical expressions for the nuclear gradient of the total excited-state energies have been derived for the algebraic diagrammatic construction scheme of the polarization propagator of up to third order. These have been implemented into a development version of the Q-Chem program package and have been used for excited-state geometry optimization of the S_1 states of the diatomics N_2, CO, and BF as well as the organic molecules *s-trans*-butadiene, *s-trans*-acrolein, and *s-trans*-(2,2′)-bithiophene. The calculated S_1 equilibrium geometries of the diatomics revealed ADC(2)-x to be more accurate than ADC(2) and ADC(2)-x and ADC(3) to exhibit a similar accuracy as EOM-CCSD. The computed excited-state geometries of butadiene and acrolein demonstrated clear limitations of the applicability of ADC(2), ADC(2)-x, and ADC(3) for the description of excited state potential energy surfaces. The deficiencies have been largely imputed to the underlying MP(2) and MP(3) ground state description in ADC(2), [ADC(2)-x], and ADC(3), respectively, which breaks down as soon as the excited-state geometry is distorted from one of the ground states in a way that it acquires some multireference character. For well-behaved organic molecules, such as BT, in which the S_1 state corresponds to a pure single-electron transition, all three ADC schemes are applicable and yield very similar results for the equilibrium geometry of the first excited singlet state.

One can expect ADC methods to become more and more reliable the larger the investigated organic molecule is, because the induced geometric changes in the excited state become smaller, and the MP treatment of the ground state remains reliable. In addition, the low-lying excited states of typical fluorescent organic chromophores are mostly pure single-electron excitations and thus well-described by ADC methods. The situation may change when the S_1

state has substantial double excitation character, as the famous $2A_g^-$ state of linear polyenes, or photo-induced reactions occur involving bond-breaking or conical intersections. Then, care must be taken and the applicability and accuracy of ADC methods need to be individually evaluated.

SUPPLEMENTARY MATERIAL

See supplementary material for the details of the comparison of the implemented analytical derivatives with values obtained from finite differences.

APPENDIX: EXPLICIT EXPRESSIONS FOR THE LAGRANGE MULTIPLIERS AND EFFECTIVE ONE- AND TWO-PARTICLE DENSITY MATRICES

First, to demonstrate how the expressions for the density matrices can be obtained for the evaluation of the analytical nuclear gradient, the expressions up to ADC(2) are derived, starting from the excitation energy in terms of the excited state vectors. All expressions presented in this section are derived from the equations published for ADC(2),[3] ADC(2)-x,[3] and ADC(3)[5] as they are implemented in the adcman module[4,6,49] embedded in the Q-Chem package of programs.[48] The final expressions for the Lagrange multipliers and the effective density matrices for the different methods are compiled in Tables VII–X.

All quantities are assumed to be real in this section. Thus, the following symmetry rules apply to the two-electron integrals and the two-particle density matrices:

$$\langle pq||rs\rangle = -\langle qp||rs\rangle = \langle qp||sr\rangle = \langle rs||pq\rangle \tag{A1}$$

and

$$\Gamma_{pqrs} = -\Gamma_{qprs} = \Gamma_{qpsr} = \Gamma_{rspq}. \tag{A2}$$

Using Eqs. (A1) and (A2), the sum

$$\sum_{pqrs} \Gamma_{pqrs}\langle pq||rs\rangle \tag{A3}$$

can be split into six canonical blocks,

$$\sum_{pqrs} \Gamma_{pqrs}\langle pq||rs\rangle = \sum_{ijkl} \Gamma_{ijkl}\langle ij||kl\rangle + 4\sum_{ijka} \Gamma_{ijka}\langle ij||ka\rangle$$
$$+ 2\sum_{ijab} \Gamma_{ijab}\langle ij||ab\rangle + 4\sum_{iajb} \Gamma_{iajb}\langle ia||jb\rangle$$
$$+ 4\sum_{iabc} \Gamma_{iabc}\langle ia||bc\rangle + \sum_{abcd} \Gamma_{abcd}\langle ab||cd\rangle. \tag{A4}$$

Recognizing the factors on the right-hand side of Eq. (A4) is important to assign the correct coefficients to the contributions of the two-particle density matrix.

Now, the expressions for the one- and two-particle density matrix are derived for ADC(2). The first order $\gamma^{ADC(1)} = \gamma^{ADC(0)}$ and $\Gamma^{ADC(1)}$ stem from the zeroth and first order contributions to $\omega^{ADC(2)}$,

TABLE VI. Intermediates and permutation operators used in Tables VII–X in addition to Eqs. (53) and (54).

$$\hat{P}_{pq}\mathcal{E}_{pq} = \mathcal{E}_{qp} \qquad\qquad \hat{P}_{pq}^{rs}\mathcal{E}_{pqrs} = \mathcal{E}_{rspq}$$

$$\gamma_{ij}^{(0)} = -\sum_c x_{jc}x_{ic} \qquad \gamma_{ab}^{(0)} = \sum_k x_{ka}x_{kb} \qquad \Gamma_{iajb}^{(1)} = x_{ia}x_{jb}$$

$$t_{iajb}^2 = \sum_{kc} t_{ikac}t_{jkbc} \qquad t_{abcd}^2 = \sum_{kl} t_{klab}t_{klcd} \qquad t_{ijkl}^2 = \sum_{cd} t_{ijcd}t_{klcd}$$

$$\rho_{ij}^{(2)} = \frac{1}{2}\sum_{kab} t_{ikab}t_{jkab} \qquad \rho_{ab}^{(2)} = \frac{1}{2}\sum_{ijc} t_{ijac}t_{ijbc} \qquad r_{ia}^x = \sum_{jb} x_{jb}t_{ijab}$$

$$\omega^{ADC(1)} = \sum_{ab} f_{ab}\sum_i x_{ia}x_{ib} - \sum_{ij} f_{ji}\sum_a x_{ia}x_{ja} - \sum_{ijab}\langle ia||jb\rangle x_{ja}x_{ib}$$
$$= \sum_{pq} f_{pq}\gamma_{pq}^{ADC(1)} + \frac{1}{4}\sum_{pqrs}\langle pq||rs\rangle\Gamma_{pqsr}^{ADC(1)}, \tag{A5}$$

and it is obvious that

$$\gamma_{ab}^{(0)} = \gamma_{ab}^{ADC(0)} = \gamma_{ab}^{ADC(1)} = \sum_k x_{ka}x_{kb},$$
$$\gamma_{ij}^{(0)} = \gamma_{ij}^{ADC(0)} = \gamma_{ij}^{ADC(1)} = -\sum_c x_{jc}x_{ic}, \tag{A6}$$
$$\Gamma_{iajb}^{ADC(1)} = -x_{ja}x_{ib}.$$

The density matrices for the correlated part of the total ADC(2) energy are defined by

$$E^{(2)} + \omega^{ADC(2)} + R_A^{ADC(2)} = \sum_{pq} f_{pq}\gamma_{pq}^{ADC(2)} + \frac{1}{4}\sum_{pqrs}\langle pq||rs\rangle\Gamma_{pqrs}^{ADC(2)}. \tag{A7}$$

The first term on the left-hand side comprises the ground-state energy, and it can readily be seen that its contribution to the occupied-occupied-virtual-virtual part of the 2RDM is $-\frac{1}{2}t_{ijab}$. The third term, $R_A^{ADC(2)}$, contains the Lagrange multipliers $\bar{t}$, which read

$$R_A^{ADC(2)} = \sum_{ijab}\bar{t}_{ijab}\left(t_{ijab}\left(\sum_c f_{ac} + \sum_c f_{bc} - \sum_k f_{ik} - \sum_k f_{jk}\right) - \langle ij||ab\rangle\right). \tag{A8}$$

Resorting the indices in Eq. (A8) yields

$$R_A^{ADC(2)} = -\sum_{ijab}\langle ij||ab\rangle\bar{t}_{ijab} + \sum_{ab} f_{ab}\sum_{ijc}\left(\bar{t}_{ijbc}t_{ijac} + \bar{t}_{ijac}t_{ijbc}\right)$$
$$- \sum_{ij} f_{ij}\sum_{kab}\left(\bar{t}_{jkab}t_{ikab} + \bar{t}_{ikab}t_{jkab}\right). \tag{A9}$$

The second order contribution to the excitation energy comprises four distinct terms

TABLE VII. Expressions for the one- and two-particle density matrices for ADC(1).

$$\gamma_{ij}^{ADC(1)} = \gamma_{ij}^{ADC(0)} = -\sum_c x_{jc}x_{ic}$$
$$\gamma_{ab}^{ADC(1)} = \gamma_{ab}^{ADC(0)} = \sum_k x_{ka}x_{kb}$$
$$\Gamma_{iajb}^{ADC(1)} = -x_{ja}x_{ib}$$

TABLE VIII. Expressions for the one- and two-particle density matrices for ADC(2) and ADC(2)-x.

$$\gamma_{ij}^{ADC(2)-x} = \gamma_{ij}^{ADC(2)} = \gamma_{ij}^{(0)} - 2\sum_{kab} x_{jkab} x_{ikab} - \left(1 + \hat{P}_{ij}\right)\sum_{kab} \bar{t}_{ikab} t_{jkab}$$

$$\gamma_{ab}^{ADC(2)-x} = \gamma_{ab}^{ADC(2)} = \gamma_{ab}^{(0)} + 2\sum_{ijc} x_{ijac} x_{ijbc} + \left(1 + \hat{P}_{ab}\right)\sum_{ijc} \bar{t}_{ijac} t_{ijbc}$$

$$\Gamma_{iajb}^{ADC(2)} = \Gamma_{iajb}^{ADC(1)} = x_{ja} x_{ib}$$

$$\Gamma_{iajb}^{ADC(2)-x} = \Gamma_{iajb}^{ADC(2)} - 4\sum_{kc} x_{ikbc} x_{jkac}$$

$$\Gamma_{ijab}^{ADC(2)-x} = \Gamma_{ijab}^{ADC(2)} = -\frac{1}{2}\left(t_{ijab} + 4\bar{t}_{ijab} + \left(1 - \hat{P}_{ab}\right)\sum_c t_{ijbc}\gamma_{ca}^{(0)} \right.$$
$$\left. - \left(1 - \hat{P}_{ij}\right)\sum_k \gamma_{jk}^{(0)} t_{ikab} + \left(1 - \hat{P}_{ij}\right)\left(1 - \hat{P}_{ab}\right) x_{ia} r_{jb}^x \right)$$

$$\Gamma_{ijka}^{ADC(2)-x} = \Gamma_{ijka}^{ADC(2)} = -2\sum_b x_{kb} x_{ijab}$$

$$\Gamma_{iabc}^{ADC(2)-x} = \Gamma_{iabc}^{ADC(2)} = -2\sum_j x_{ja} x_{ijbc}$$

$$\Gamma_{ijkl}^{ADC(2)-x} = 2\sum_{ab} x_{ijab} x_{klab}$$

$$\Gamma_{abcd}^{ADC(2-x)} = 2\sum_{ij} x_{ijcd} x_{ijab}$$

$$\bar{t}_{ijab} = \frac{1}{\epsilon_a + \epsilon_b - \epsilon_i - \epsilon_j}\left(\langle ij\|ab\rangle + \left(1 - \hat{P}_{ab}\right)\sum_c \langle ij\|bc\rangle\gamma_{ac}^{(0)} - \left(1 - \hat{P}_{ij}\right)\sum_k \langle jk\|ab\rangle\gamma_{ik}^{(0)} \right.$$
$$\left. + \left(1 - \hat{P}_{ij}\right)\left(1 - \hat{P}_{ab}\right) x_{ia}\sum_{ck} \langle jk\|bc\rangle x_{kc} \right)$$

$$\omega^{(2)} = \omega_{11} + \omega_{12} + \omega_{21} + \omega_{22}. \tag{A10}$$

The first one, ω_{11}, is given as

$$\omega_{11} = \frac{1}{4}\sum_{ab}\left(\sum_{klc} t_{klac}\langle kl\|bc\rangle + \sum_{klc}\langle kl\|ac\rangle t_{klbc} \right)\sum_i x_{ia} x_{ib}$$
$$+ \frac{1}{4}\sum_{ij}\left(\sum_{kcd} t_{ikcd}\langle |cd\rangle + \sum_{kcd}\langle ik\|cd\rangle t_{jkcd} \right)\sum_a x_{ia} x_{ja}$$
$$- \frac{1}{2}\sum_{ijab}\left(\sum_{kc} t_{ikac}\langle |bc\rangle + \sum_{kc}\langle ik\|ac\rangle t_{jkbc} \right) x_{ia} x_{jb}. \tag{A11}$$

Again, by resorting the indices and using the derived expressions above for $\gamma^{(0)}$, one finds

$$\omega_{11} = +\sum_{ijab}\langle ij\|ab\rangle\frac{1}{4}\left(\sum_c t_{ijcb}\gamma_{ca}^{(0)} - \sum_c t_{ijca}\gamma_{cb}^{(0)} \right)$$
$$- \sum_{ijab}\langle ij\|ab\rangle\frac{1}{4}\left(\sum_k \gamma_{ik}^{(0)} t_{kjab} - \sum_k \gamma_{jk}^{(0)} t_{kiab} \right)$$
$$- \sum_{ijab}\langle ij\|ab\rangle\frac{1}{4}\left(x_{ia}\sum_{kc} t_{jkbc} x_{kc} - x_{ja}\sum_{kc} t_{ikbc} x_{kc} \right.$$
$$\left. - x_{ib}\sum_{kc} t_{jkac} x_{kc} + x_{jb}\sum_{kc} t_{ikac} x_{kc} \right). \tag{A12}$$

The next two contributions to $\omega^{(2)}$,

$$\omega_{12} = \sum_{ijka}\langle ij\|ka\rangle\sum_b x_{kb} x_{ijba} + \sum_{iabc}\langle ia\|bc\rangle\sum_j x_{ja} x_{jibc} \tag{A13}$$

TABLE IX. Expressions for the one-particle density for ADC(3).

$$\gamma_{ij}^{ADC(3)} = \gamma_{ij}^{(0)} - 2\sum_{kab} x_{jkab} x_{ikab}$$
$$- \left(1 + \hat{P}_{ij}\right)\left(\sum_{kab} \bar{t}_{ikab} t_{jkab} + \sum_{kab} \bar{T}_{ikab}^D T_{jkab}^D + \frac{1}{2}\sum_a \bar{\rho}_{ia}\rho_{ja}^{(2)} \right)$$
$$\gamma_{ab}^{ADC(3)} = \gamma_{ab}^{(0)} + 2\sum_{ijc} x_{ijac} x_{ijbc}$$
$$+ \left(1 + \hat{P}_{ab}\right)\left(\sum_{ijc} \bar{t}_{ijac} t_{ijbc} + \sum_{ijc} \bar{T}_{ijac}^D T_{ijbc}^D + \frac{1}{2}\sum_i \bar{\rho}_{ia}\rho_{ib}^{(2)} \right)$$

and

$$\omega_{21} = \sum_{ijka} \langle ia||jk\rangle \sum_b x_{jkba} x_{ib} + \sum_{iabc} \langle ab||ic\rangle \sum_j x_{jiab} x_{jc}, \tag{A14}$$

can be summed up to yield

$$\omega_{12} + \omega_{21} = 2\sum_{ijka} \langle ij||ka\rangle \sum_b x_{kb} x_{ijba} + 2\sum_{iabc} \langle ia||bc\rangle \sum_j x_{ja} x_{jibc}, \tag{A15}$$

and the last contribution reads

$$\omega_{22} = 2\sum_{ab} f_{ab} \sum_{ijc} x_{ijac} x_{ijbc} - 2\sum_{ij} f_{ji} \sum_{kab} x_{ikab} x_{jkab}. \tag{A16}$$

As a result, we can identify the one- and two-particle density matrices for ADC(2) including the zeroth- and first-order contributions

from Eq. (A6) as

$$\gamma_{ab}^{ADC(2)} = \gamma_{ab}^{(0)} + \left(1 + \hat{\mathcal{P}}_{ab}\right) \sum_{ijc} \tilde{t}_{ijbc} t_{ijac} + 2\sum_{ijc} x_{ijac} x_{ijbc}, \tag{A17}$$

$$\gamma_{ij}^{ADC(2)} = \gamma_{ij}^{(0)} - \left(1 + \hat{\mathcal{P}}_{ij}\right) \sum_{kab} \tilde{t}_{jkab} t_{ikab} - 2\sum_{kab} x_{jkab} x_{ikab}, \tag{A18}$$

and

$$\begin{aligned}
\Gamma_{ijab}^{ADC(2)} = &-\frac{1}{2} t_{ijab} - 2\tilde{t}_{ijab} \\
&-\frac{1}{2}\left(1 - \hat{\mathcal{P}}_{ab}\right) \sum_c t_{ijbc} \gamma_{ca}^{(0)} + \frac{1}{2}\left(1 - \hat{\mathcal{P}}_{ij}\right) \sum_k \gamma_{ik}^{(0)} t_{jkab} \\
&-\frac{1}{2}\left(1 - \hat{\mathcal{P}}_{ij}\right)\left(1 - \hat{\mathcal{P}}_{ab}\right) x_{ia} \sum_{kc} t_{jkbc} x_{kc},
\end{aligned} \tag{A19}$$

TABLE X. Expressions the two-particle density matrix for ADC(3).

$$\begin{aligned}
\Gamma_{ijkl}^{ADC(3)} =& 2\sum_{ab} x_{ijab} x_{klab} + \frac{1}{2}\left(1 + \hat{\mathcal{P}}_{ij}^{kl}\right)\Bigg(2\sum_{ab} \bar{T}_{ijab}^D t_{klab} + \frac{1}{2}\left(1 - \hat{\mathcal{P}}_{ij}\right)\sum_m \gamma_{jm}^{(0)} t_{imkl}^2 \\
&+ \left(1 - \hat{\mathcal{P}}_{kl}\right)\sum_c x_{kc} \sum_b t_{ijbc} r_{lb}^x + \left(1 - \hat{\mathcal{P}}_{ij}\right)\left(1 - \hat{\mathcal{P}}_{kl}\right)\left(\rho_{jl}^{(2)} \gamma_{ik}^{(0)} - \sum_{ab} t_{lajb}^2 \Gamma_{iakb}^{(1)}\right)\Bigg)
\end{aligned}$$

$$\begin{aligned}
\Gamma_{ijka}^{ADC(3)} =& -2\sum_b x_{kb} x_{ijab} - \sum_l x_{la} \sum_{bc} t_{ijab} x_{klbc} + \left(1 - \hat{\mathcal{P}}_{ij}\right)\Bigg(2\sum_c x_{ic} \sum_{lb} t_{jlab} x_{klbc} \\
&- x_{ja} \sum_{lbc} t_{ilbc} x_{klbc} + \rho_{ja}^{(2)} \gamma_{ik}^{(0)} + x_{ia} \sum_b \rho_{jb}^{(2)} x_{kb} - \frac{1}{2}\sum_b t_{ijab} \bar{\rho}_{kb}\Bigg)
\end{aligned}$$

$$\begin{aligned}
\Gamma_{ijab}^{ADC(3)} =& \frac{1}{2}\Bigg(-t_{ijab} - t_{ijab}^D - 4\tilde{t}_{ijab} - \left(1 - \hat{\mathcal{P}}_{ab}\right)\sum_c \left(T_{ijbc}^D + t_{ijbc}\right)\gamma_{ac}^{(0)} \\
&+ \left(1 - \hat{\mathcal{P}}_{ij}\right)\sum_k \left(T_{jkab}^D + t_{jkab}\right)\gamma_{ik}^{(0)} - \left(1 - \hat{\mathcal{P}}_{ab}\right)\left(1 - \hat{\mathcal{P}}_{ij}\right)x_{ia}\left(\sum_{kc} T_{jkbc}^D x_{kc} + r_{jb}^x\right)\Bigg)
\end{aligned}$$

$$\begin{aligned}
\Gamma_{iajb}^{ADC(3)} =& -\Gamma_{jaib}^{(1)} - 4\sum_{kc} x_{ikbc} x_{jkac} + \rho_{ij}^{(2)} \gamma_{ab}^{(0)} + \rho_{ab}^{(2)} \gamma_{ij}^{(0)} + \frac{1}{2}\left(1 + \hat{\mathcal{P}}_{ia}^{jb}\right)\Bigg(-4\sum_{kc} t_{ikbc} \bar{T}_{jkac}^D \\
&+ 4\sum_c t_{ibjc}^2 \gamma_{ac}^{(0)} - \sum_k t_{ibka}^2 \gamma_{jk}^{(0)} + \sum_k x_{ka} \sum_d t_{ikbc} r_{jc}^x + \sum_k x_{jc} \sum_l t_{ikbc} r_{ka}^x \\
&+ x_{ja} \sum_c \rho_{cb}^{(2)} x_{ic} - x_{ib} \sum_k \rho_{jk}^{(2)} x_{ka} - 2\sum_{kc} t_{jckb}^2 \Gamma_{icka}^{(1)} \\
&+ \frac{1}{2}\sum_{cd} t_{acbd}^2 \Gamma_{icjd}^{(1)} + \frac{1}{2}\sum_{kl} t_{ikjl}^2 \Gamma_{kalb}^{(1)}\Bigg)
\end{aligned}$$

$$\begin{aligned}
\Gamma_{iabc}^{ADC(3)} =& -2\sum_j x_{ja} x_{ijbc} + \sum_d x_{id} \sum_{jk} t_{jkbc} x_{jkad} + \left(1 - \hat{\mathcal{P}}_{bc}\right)\Bigg(-2\sum_j x_{jb} \sum_{kd} t_{ikcd} x_{jkad} \\
&+ x_{ib} \sum_{jkd} t_{jkcd} x_{jkad} - \rho_{ic}^{(2)} \gamma_{ab}^{(0)} + x_{ib} \sum_j \rho_{jc}^{(2)} x_{ja} - \frac{1}{2}\sum_b t_{ijbc} \bar{\rho}_{ja}\Bigg)
\end{aligned}$$

$$\begin{aligned}
\Gamma_{abcd}^{ADC(3)} =& 2\sum_{ij} x_{ijcd} x_{ijab} + \frac{1}{2}\left(1 + \hat{\mathcal{P}}_{ab}^{cd}\right)\Bigg(2\sum_{ij} \bar{T}_{ijab}^D t_{ijcd} + \frac{1}{2}\left(1 - \hat{\mathcal{P}}_{ab}\right)\sum_e \gamma_{eb}^{(0)} t_{aecd}^2 \\
&+ \left(1 - \hat{\mathcal{P}}_{ab}\right)\sum_i x_{ia} \sum_j t_{jkcd} r_{jb}^x + \left(1 - \hat{\mathcal{P}}_{ab}\right)\left(1 - \hat{\mathcal{P}}_{cd}\right)\left(\rho_{bd}^{(2)} \gamma_{ac}^{(0)} - \sum_{ij} t_{idjb}^2 \Gamma_{iajc}^{(1)}\right)\Bigg)
\end{aligned}$$

TABLE XI. Expressions for the ADC(3) amplitude Lagrange multipliers.

$$\bar{t}_{ijab} = \frac{\langle ij||ab\rangle + \sum_{n=1}^{6}{}^{n}\bar{t}_{ijab} + \bar{t}_{ijab}^{TD} + \bar{t}_{ijab}^{\rho}}{\epsilon_a + \epsilon_b - \epsilon_i - \epsilon_j}$$

$${}^{1}\bar{t}_{ijab} = -\sum_{kl} t_{klab} \sum_m \langle ij||km\rangle \gamma_{lm}^{(0)} - \left(1 - \hat{P}_{ab}\right) \sum_k x_{ka} \sum_l \langle ij||kl\rangle r_{lb}^{x}$$

$$+ \left(1 - \hat{P}_{ij}\right)\left(\frac{1}{2}\sum_k \gamma_{ik}^{(0)} \sum_{lm} \langle jk||lm\rangle t_{lmab} - 2\sum_k t_{jkab} \sum_{lm} \gamma_{lm}^{(0)} \langle il||km\rangle\right)$$

$$- \left(1 - \hat{P}_{ij}\right)\left(1 - \hat{P}_{ab}\right)\left(\frac{1}{2}x_{ia}\sum_{kc}x_{kc}\sum_{lm}\langle jk||lm\rangle t_{lmbc} - \sum_k x_{ka}\sum_{lm}\langle li||km\rangle\sum_c t_{jmbc}x_{mc}\right)$$

$${}^{2}\bar{t}_{ijab} = 4\left(-\sum_{kc}\langle ij||kc\rangle\sum_l x_{lc}x_{klab} + \left(1 - \hat{P}_{ij}\right)\sum_k x_{ikab}\sum_{kc}\langle jl||kc\rangle x_{lc}\right.$$

$$\left. - \left(1 - \hat{P}_{ij}\right)\left(1 - \hat{P}_{ab}\right)\sum_{kl}\langle jk||lb\rangle\sum_c x_{kc}x_{ilac}\right)$$

$${}^{3}\bar{t}_{ijab} = \left(1 - \hat{P}_{ab}\right)\sum_c\langle ij||bc\rangle\gamma_{ac}^{(0)} - \left(1 - \hat{P}_{ij}\right)\sum_k\langle jk||ab\rangle\gamma_{ik}^{(0)}$$

$$+ \left(1 - \hat{P}_{ij}\right)\left(1 - \hat{P}_{ab}\right)x_{ia}\sum_{kc}\langle jk||bc\rangle x_{kc}$$

$${}^{4}\bar{t}_{ijab} = \left(1 - \hat{P}_{ij}\right)\left(-2\sum_k t_{jkab}\sum_{cd}\langle ic||kd\rangle\gamma_{cd}^{(0)} - 2\sum_{kl}t_{klab}\sum_{cd}\Gamma_{ickd}^{(1)}\langle jc||ld\rangle\right.$$

$$\left. + \sum_c x_{ic}\sum_k t_{jkab}\sum_{ld}x_{ld}\langle lc||kd\rangle + \sum_k t_{jkab}\sum_c x_{kc}\sum_{ld}x_{ld}\langle lc||id\rangle\right)$$

$$+ \left(1 - \hat{P}_{ab}\right)\left(-2\sum_c t_{ijcb}\sum_{kl}\langle ka||lc\rangle\gamma_{kl}^{(0)} - 2\sum_{cd}t_{ijcd}\sum_{kl}\Gamma_{kalc}^{(1)}\langle kb||ld\rangle\right.$$

$$\left. + \sum_k x_{ka}\sum_c t_{ijbc}\sum_{ld}x_{ld}\langle kd||lc\rangle + \sum_c t_{ijbc}\sum_k x_{kc}\sum_{ld}x_{ld}\langle kd||la\rangle\right)$$

$$+ \left(1 - \hat{P}_{ij}\right)\left(1 - \hat{P}_{ab}\right)\left(\sum_c\gamma_{ac}^{(0)}\sum_{kc}\langle kc||jd\rangle t_{ikbd} - \sum_{kc}\langle jc||kb\rangle\sum_d t_{ikad}\gamma_{cd}^{(0)}\right.$$

$$- \sum_k\gamma_{ik}^{(0)}\sum_{lc}\langle lb||kc\rangle t_{jlac} + \sum_{kc}\langle jc||kb\rangle\sum_l t_{ilac}\gamma_{kl}^{(0)} - \sum_c x_{ic}\sum_k\langle jc||kb\rangle r_{ka}^{x}$$

$$- x_{jb}\sum_{kc}x_{kc}\sum_{ld}\langle lc||id\rangle t_{klad} - \sum_k x_{ka}\sum_c\langle jc||kb\rangle r_{ic}^{x} - x_{jb}\sum_{kc}x_{kc}\sum_{ld}\langle la||kd\rangle t_{ilcd}$$

$$\left. + 2\sum_{cd}\left(\sum_k x_{ka}\langle ic||kd\rangle\right)\left(\sum_l x_{lc}t_{jlbd}\right) + 2\sum_{kl}\left(\sum_c x_{ic}\langle kc||la\rangle\right)\left(\sum_d x_{kd}t_{ljdb}\right)\right)$$

$${}^{5}\bar{t}_{ijab} = -4\left(\sum_{kc}\langle kc||ab\rangle\sum_d x_{kd}x_{ijcd} + \left(1 - \hat{P}_{ab}\right)\sum_c x_{ijbc}\sum_{kd}\langle kc||ad\rangle x_{kd}\right.$$

$$\left. + \left(1 - \hat{P}_{ij}\right)\left(1 - \hat{P}_{ab}\right)\sum_{cd}\langle jc||bd\rangle\sum_k x_{kd}x_{ikac}\right)$$

$${}^{6}\bar{t}_{ijab} = -\sum_{cd}t_{ijcd}\sum_e\langle ab||de\rangle\gamma_{ce}^{(0)} - \left(1 - \hat{P}_{ij}\right)\sum_c x_{ic}\sum_d\langle ab||cd\rangle\sum_{ke}t_{jkde}x_{ke}$$

$$- \left(1 - \hat{P}_{ab}\right)\left(\frac{1}{2}\sum_c\gamma_{ac}^{(0)}\sum_{de}\langle bc||de\rangle t_{ijde} - 2\sum_c t_{ijbc}\sum_{de}\gamma_{de}^{(0)}\langle ad||ce\rangle\right)$$

$$- \left(1 - \hat{P}_{ij}\right)\left(1 - \hat{P}_{ab}\right)\left(\frac{1}{2}x_{ia}\sum_{kc}x_{kc}\sum_{de}\langle bc||de\rangle t_{jkde} - 2\sum_c x_{ic}\sum_{de}\langle ad||ce\rangle\sum_k t_{jkeb}x_{kd}\right)$$

TABLE XI. (*Continued.*)

$$\tilde{t}_{ijab}^{T^D} = 2\left(1 - \hat{P}_{ij}\right)\left(1 - \hat{P}_{ab}\right)\left(2\sum_{kc}\bar{T}_{ikac}^D\langle jc||kb\rangle - \sum_{cd}\bar{T}_{ijcd}^D\langle ab||cd\rangle - \sum_{kl}\bar{T}_{klab}^D\langle ij||kl\rangle\right)$$

$$\tilde{t}_{ijab}^{\rho} = -\left(1 - \hat{P}_{ij}\right)\sum_c\langle jc||ab\rangle\bar{\rho}_{ic} - \left(1 - \hat{P}_{ab}\right)\sum_k\langle ij||kb\rangle\bar{\rho}_{ka}$$

$$\bar{T}_{ijab}^D = \left(1 - \hat{P}_{ab}\right)\sum_c\langle ij||bc\rangle\gamma_{ac}^{(0)} - \left(1 - \hat{P}_{ij}\right)\sum_k\langle jk||ab\rangle\gamma_{ik}^{(0)} + \left(1 - \hat{P}_{ij}\right)\left(1 - \hat{P}_{ab}\right)x_{ia}\sum_{ck}\langle jk||bc\rangle x_{kc}$$

$$\bar{\rho}_{ia} = \frac{2}{\epsilon_a - \epsilon_i}\left(\sum_{jk}\langle ij||ka\rangle\gamma_{jk}^{(0)} + \sum_{jb}x_{jb}\sum_k x_{ka}\langle ij||kb\rangle - \sum_{bc}\langle ic||ab\rangle\gamma_{bc}^{(0)} + \sum_{jb}x_{jb}\sum_c x_{ic}\langle jc||ab\rangle\right)$$

$$\Gamma_{ijka}^{ADC(2)} = 2\sum_b x_{kb}x_{ijba}, \quad \Gamma_{iabc}^{ADC(2)} = 2\sum_j x_{ja}x_{jibc}, \tag{A20}$$

$$\Gamma_{iajb}^{ADC(2)} = \Gamma_{iajb}^{ADC(1)}. \tag{A21}$$

The explicit form of $\bar{t}$ for ADC(2) is given in Eq. (62) and again in Table VIII. For the evaluation of the ADC(2)-x energy derivatives, only additional terms in the Γ_{ijkl}, Γ_{abcd}, and Γ_{iajb} blocks of the two-particle density matrix are required. The same procedure has been used to derive the expressions for the density matrices and Lagrange multipliers for ADC(2)-x and ADC(3). Table VI contains expressions for intermediates and permutation operators that are used in Tables VII–XI.

REFERENCES

[1] P. Pulay, "*Ab initio* calculation of force constants and equilibrium geometries in polyatomic molecules," Mol. Phys. **17**, 197–204 (1969).

[2] P. Pulay, "Analytical derivatives, forces, force constants, molecular geometries, and related response properties in electronic structure theory," Wiley Interdiscip. Rev.: Comput. Mol. Sci. **4**, 169–181 (2014).

[3] J. Schirmer, Phys. Rev. A **26**, 2395 (1982).

[4] A. Dreuw and M. Wormit, "The algebraic diagrammatic construction scheme for the polarization propagator for the calculation of excited states," Wiley Interdiscip. Rev.: Comput. Mol. Sci. **5**, 82–95 (2015).

[5] A. B. Trofimov, G. Stelter, and J. Schirmer, J. Chem. Phys. **111**, 9982 (1999).

[6] P. H. P. Harbach, M. Wormit, and A. Dreuw, "The third-order algebraic diagrammatic construction method (ADC(3)) for the polarization propagator for closed-shell molecules: Efficient implementation and benchmarking," J. Chem. Phys. **141**, 064113 (2014).

[7] O. Christiansen, H. Koch, and P. Jørgensen, Chem. Phys. Lett. **243**, 409 (1995).

[8] C. Møller and M. S. Plesset, Phys. Rev. **46**, 618 (1934).

[9] H. Hellmann, *Einführung in die Quantenchemie* (Franz Deuticke, Leipzig, 1937).

[10] R. P. Feynman, "Forces in molecules," Phys. Rev. **56**, 340–343 (1939).

[11] N. C. Handy and H. F. Schaefer III, "On the evaluation of analytic energy derivatives for correlated wave functions," J. Chem. Phys. **81**, 5031–5033 (1984).

[12] T. Helgaker and P. Jørgensen, "Configuration-interaction energy derivatives in a fully variational formulation," Theor. Chim. Acta **75**, 111–127 (1989).

[13] W. Weber and W. Thiel, Theor. Chem. Acc. **103**, 495 (2000).

[14] A. Koslowski, M. E. Beck, and W. Thiel, "Implementation of a general multireference configuration interaction procedure with analytic gradients in a semiempirical context using the graphical unitary group approach," J. Comput. Chem. **24**, 714–726 (2003).

[15] H. Lischka, R. Shepard, R. M. Pitzer, I. Shavitt, M. Dallos, T. Müller, P. G. Szalay, M. Seth, G. S. Kedziora, S. Yabushita, and Z. Zhang, "High-level multireference methods in the quantum-chemistry program system COLUMBUS: Analytic MR-CISD and MR-AQCC gradients and MR-AQCC-LRT for excited states, GUGA spin-orbit CI and parallel CI density," Phys. Chem. Chem. Phys. **3**, 664 (2001).

[16] G. Cui and W. Thiel, "Generalized trajectory surface-hopping method for internal conversion and intersystem crossing," J. Chem. Phys. **141**, 124101 (2014).

[17] M. Barbatti, M. Ruckenbauer, F. Plasser, J. Pittner, G. Granucci, M. Persico, and H. Lischka, "Newton-X: A surface-hopping program for nonadiabatic molecular dynamics," Wiley Interdiscip. Rev.: Comput. Mol. Sci. **4**, 26–33 (2014).

[18] E. Runge and E. K. U. Gross, Phys. Rev. Lett. **52**, 997–1000 (1984).

[19] M. E. Casida, *Recent Advances in Density Functional Methods, Part I* (World Scientific, Singapore, 1995), pp. 155–192.

[20] A. Dreuw and M. Head-Gordon, Chem. Rev. **105**, 4009–4037 (2005).

[21] F. Furche and R. Ahlrichs, "Adiabatic time-dependent density functional methods for excited state properties," J. Chem. Phys. **117**, 7433–7447 (2002).

[22] M. Chiba, T. Tsuneda, and K. Hirao, "Excited state geometry optimizations by analytical energy gradient of long-range corrected time-dependent density functional theory," J. Chem. Phys. **124**, 144106 (2006).

[23] T. Petrenko, S. Kossmann, and F. Neese, "Efficient time-dependent density functional theory approximations for hybrid density functionals: Analytical gradients and parallelization," J. Chem. Phys. **134**, 054116 (2011).

[24] F. Liu, Z. Gan, Y. Shao, C. P. Hsu, A. Dreuw, M. Head-Gordon, B. T. Miller, B. R. Brooks, J. G. Yu, T. R. Furlani, and J. Kong, "A parallel implementation of the analytic nuclear gradient for time-dependent density functional theory within the Tamm-Dancoff approximation," Mol. Phys. **108**, 2791 (2010).

[25] P. J. Bruna and S. D. Peyerimhoff, "Excited-state potentials," in *Advances in Chemical Physics* (Wiley, 2007), pp. 1–97.

[26] R. McWeeny and B. T. Sutcliffe, *Methods of Molecular Quantum Mechanics* (Academic Press, London, 1969).

[27] Y. Osamura, Y. Yamaguchi, and H. F. Schaefer, "Generalization of analytic configuration interaction (CI) gradient techniques for potential energy hypersurfaces, including a solution to the coupled perturbed Hartree–Fock equations for multiconfiguration SCF molecular wave functions," J. Chem. Phys. **77**, 383 (1982).

[28] M. G. Delcey, L. Freitag, T. B. Pedersen, F. Aquilante, R. Lindh, and L. González, "Analytical gradients of complete active space self-consistent field energies using Cholesky decomposition: Geometry optimization and spin-state energetics of a ruthenium nitrosyl complex," J. Chem. Phys. **140**, 174103 (2014).

[29] J. W. Snyder, E. G. Hohenstein, N. Luehr, and T. J. Martínez, "An atomic orbital-based formulation of analytical gradients and nonadiabatic coupling vector elements for the state-averaged complete active space self-consistent field method on graphical processing units," J. Chem. Phys. **143**, 154107 (2015).

[30] P. Celani and H.-J. Werner, "Analytical energy gradients for internally contracted second-order multireference perturbation theory," J. Chem. Phys. **119**, 5044 (2003).

[31] B. Vlaisavljevich and T. Shiozaki, "Nuclear energy gradients for internally contracted complete active space second-order perturbation theory: Multistate extensions," J. Chem. Theory Comput. **12**, 3781 (2016); e-print arXiv:1606.01273.

[32] C. Haettig and F. Weigend, "CC2 excitation energy calculations on large molecules using the resolution of the identity approximation," J. Chem. Phys. **113**, 5154 (2000).

[33] A. Köhn and C. Hättig, "Analytic gradients for excited states in the coupled-cluster model CC2 employing the resolution-of-the-identity approximation," J. Chem. Phys. **119**, 5021 (2003).

[34] C. Hättig, "Structure optimizations for excited states with correlated second-order methods: CC2 and ADC(2)," Adv. Quantum Chem. **50**, 37 (2005).

[35] K. Ledermüller and M. Schütz, "Local CC2 response method based on the Laplace transform: Analytic energy gradients for ground and excited states," J. Chem. Phys. **140**, 164113 (2014).

[36] S. V. Levchenko, T. Wang, and A. I. Krylov, "Analytic gradients for the spin-conserving and spin-flipping equation-of-motion coupled-cluster models with single and double substitutions," J. Chem. Phys. **122**, 224106 (2005).

[37] H. Sekino and R. J. Bartlett, Int. J. Quant. Chem. Symp. **26**, 255 (1984).

[38] J. F. Stanton and R. J. Bartlett, J. Chem. Phys. **98**, 7029 (1993).

[39] E. Dalgaard and H. J. Monkhorst, Phys. Rev. A **28**, 1217 (1983).

[40] H. Koch and P. Jørgensen, J. Chem. Phys. **93**, 3333 (1990).

[41] J. F. Stanton and J. Gauss, "Analytic energy derivatives for ionized states described by the equation-of-motion coupled cluster method," J. Chem. Phys. **101**, 8938 (1994).

[42] J. F. Stanton and J. Gauss, "Analytic energy gradients for the equation-of-motion coupled-cluster method: Implementation and application to the HCN/HNC system," J. Chem. Phys. **100**, 4695 (1994).

[43] M. Kállay and J. Gauss, "Calculation of excited-state properties using general coupled-cluster and configuration-interaction models," J. Chem. Phys. **121**, 9257 (2004).

[44] J. Schirmer and A. B. Trofimov, J. Chem. Phys. **120**, 11449 (2004).

[45] J. Schirmer and G. Angonoa, "On green's function calculations of the static self-energy part, the ground state energy and expectation values," J. Chem. Phys. **91**, 1754–1761 (1989).

[46] M. J. Frisch, M. Head-Gordon, and J. A. Pople, "A direct MP2 gradient method," Chem. Phys. Lett. **166**, 275–280 (1990).

[47] J. Gauss and D. Cremer, "Implementation of analytical energy gradients at third- and fourth-order Møller-Plesset perturbation theory," Chem. Phys. Lett. **138**, 131–140 (1987).

[48] Y. Shao, Z. Gan, E. Epifanovsky, A. T. Gilbert, M. Wormit, J. Kussmann, A. W. Lange, A. Behn, J. Deng, X. Feng, D. Ghosh, M. Goldey, P. R. Horn, L. D. Jacobson, I. Kaliman, R. Z. Khaliullin, T. Kús, A. Landau, J. Liu, E. I. Proynov, Y. M. Rhee, R. M. Richard, M. A. Rohrdanz, R. P. Steele, E. J. Sundstrom, H. L. W. III, P. M. Zimmerman, D. Zuev, B. Albrecht, E. Alguire, B. Austin, G. J. O. Beran, Y. A. Bernard, E. Berquist, K. Brandhorst, K. B. Bravaya, S. T. Brown, D. Casanova, C.-M. Chang, Y. Chen, S. H. Chien, K. D. Closser, D. L. Crittenden, M. Diedenhofen, R. A. DiStasio, Jr., H. Do, A. D. Dutoi, R. G. Edgar, S. Fatehi, L. Fusti-Molnar, A. Ghysels, A. Golubeva-Zadorozhnaya, J. Gomes, M. W. Hanson-Heine, P. H. Harbach, A. W. Hauser, E. G. Hohenstein, Z. C. Holden, T.-C. Jagau, H. Ji, B. Kaduk, K. Khistyaev, J. Kim, J. Kim, R. A. King, P. Klunzinger, D. Kosenkov, T. Kowalczyk, C. M. Krauter, K. U. Lao, A. D. Laurent, K. V. Lawler, S. V. Levchenko, C. Y. Lin, F. Liu, E. Livshits, R. C. Lochan, A. Luenser, P. Manohar, S. F. Manzer, S.-P. Mao, N. Mardirossian, A. V. Marenich, S. A. Maurer, N. J. Mayhall, E. Neuscamman, C. M. Oana, R. Olivares-Amaya, D. P. O'Neill, J. A. Parkhill, T. M. Perrine, R. Peverati, A. Prociuk, D. R. Rehn, E. Rosta, N. J. Russ, S. M. Sharada, S. Sharma, D. W. Small, A. Sodt, T. Stein, D. Stück, Y.-C. Su, A. J. Thom, T. Tsuchimochi, V. Vanovschi, L. Vogt, O. Vydrov, T. Wang, M. A. Watson, J. Wenzel, A. White, C. F. Williams, J. Yang, S. Yeganeh, S. R. Yost, Z.-Q. You, I. Y. Zhang, X. Zhang, Y. Zhao, B. R. Brooks, G. K. Chan, D. M. Chipman, C. J. Cramer, W. A. Goddard III, M. S. Gordon, W. J. Hehre, A. Klamt, H. F. Schaefer III, M. W. Schmidt, C. D. Sherrill, D. G. Truhlar, A. Warshel, X. Xu, A. Aspuru-Guzik, R. Baer, A. T. Bell, N. A. Besley, J.-D. Chai, A. Dreuw, B. D. Dunietz, T. R. Furlani, S. R. Gwaltney, C.-P. Hsu, Y. Jung, J. Kong, D. S. Lambrecht, W. Liang, C. Ochsenfeld, V. A. Rassolov, L. V. Slipchenko, J. E. Subotnik, T. V. Voorhis, J. M. Herbert, A. I. Krylov, P. M. Gill, and M. Head-Gordon, "Advances in molecular quantum chemistry contained in the q-chem 4 program package," Mol. Phys. **113**, 184–215 (2015).

[49] M. Wormit, D. R. Rehn, P. H. Harbach, J. Wenzel, C. M. Krauter, E. Epifanovsky, and A. Dreuw, "Investigating excited electronic states using the algebraic diagrammatic construction (ADC) approach of the polarisation propagator," Mol. Phys. **112**, 774–784 (2014).

[50] E. Epifanovsky, M. Wormit, T. Kuś, A. Landau, D. Zuev, K. Khistyaev, P. Manohar, I. Kaliman, A. Dreuw, and A. I. Krylov, "New implementation of high-level correlated methods using a general block tensor library for high-performance electronic structure calculations," J. Comput. Chem. **34**, 2293–2309 (2013).

[51] E. R. Davidson, J. Comput. Phys. **17**, 87–94 (1975).

[52] P. Pulay, "Convergence acceleration of iterative sequences. The case of SCF iteration," Chem. Phys. Lett. **73**, 393–398 (1980).

[53] D. Rehn, Ph.D. dissertation (Universität Heidelberg, 2015).

[54] T. H. Dunning, Jr., J. Chem. Phys. **90**, 1007 (1989).

[55] D. E. Woon and T. H. Dunning, "Gaussian basis sets for use in correlated molecular calculations. IV. Calculation of static electrical response properties," J. Chem. Phys. **100**, 2975–2988 (1994).

[56] D. E. Woon and T. H. Dunning, "Gaussian basis sets for use in correlated molecular calculations. III. The atoms aluminum through argon," J. Chem. Phys. **98**, 1358–1371 (1993).

[57] F. Zhang, D. Wu, Y. Xu, and X. Feng, "Thiophene-based conjugated oligomers for organic solar cells," J. Mater. Chem. **21**, 17590–17600 (2011).

[58] D. Bélanger, "Polythiophenes as active electrode materials for electrochemical capacitors," in Handbook of Thiophene-Based Materials (John Wiley & Sons, 2009), pp. 577–594.

[59] A. Mishra, C.-Q. Ma, J. L. Segura, and P. Bäuerle, Functional Oligothiophene-Based Materials: Nanoarchitectures and Applications (John Wiley & Sons, 2009), pp. 1–155.

[60] A. Åslund, C. J. Sigurdson, T. Klingstedt, S. Grathwohl, T. Bolmont, D. L. Dickstein, E. Glimsdal, S. Prokop, M. Lindgren, P. Konradsson, D. M. Holtzman, P. R. Hof, F. L. Heppner, S. Gandy, M. Jucker, A. Aguzzi, P. Hammarström, and K. P. R. Nilsson, "Novel pentameric thiophene derivatives for in vitro and in vivo optical imaging of a plethora of protein aggregates in cerebral amyloidoses," ACS Chem. Biol. **4**, 673–684 (2009).

[61] K. P. Huber and G. Herzberg, Molecular Spectra and Molecular Structure IV. Constants of Diatomic Molecules (Van Nostrand, New York, 1979).

[62] C. S. Page and M. Olivucci, "Ground and excited state CASPT2 geometry optimizations of small organic molecules," J. Comput. Chem. **24**, 298–309 (2003).

[63] M. Rubio, M. Merchan, R. Pou-Amerigo, and E. Orti, "The low-lying excited states of 2,2'-bithiophene: A theoretical analysis," ChemPhysChem **4**, 1308–1315 (2003).

[64] J. E. Chadwick and B. E. Kohler, "Optical spectra of isolated s-cis- and s-trans-bithiophene: Torsional potential in the ground and excited states," J. Phys. Chem. **98**, 3631–3637 (1994).

[65] D. Birnbaum and B. E. Kohler, "Location of a 1ag state in bithiophene," J. Chem. Phys. **96**, 2492–2495 (1992).

[66] T. H. Dunning and K. A. Peterson, "Use of Möller-Plesset perturbation theory in molecular calculations: Spectroscopic constants of first row diatomic molecules," J. Chem. Phys. **108**, 4761–4771 (1998).